MODIFICATION OF EXPANSIVE SOIL AND REPAIR OF DAMAGED SMART CEMENT USING POLYMER

A Thesis

Presented to

the Faculty of the Department of Civil and Environmental Engineering

University of Houston

In Partial Fulfillment

Of the Requirements for the Degree

Master of Science

in Civil Engineering

by

Mythili Thevamaran

May 2017

MODIFICATION OF EXPANSIVE SOIL AND REPAIR OF DAMAGED SMART CEMENT USING POLYMER

Mythili Thevamaran

Approved:

Chair of the Committee
Cumaraswamy Vipulanandan, Professor,
Civil and Environmental Engineering

Committee Members:

Yi-Lung Mo, Professor,
Civil and Environmental Engineering

Yuhua Chen, Associate Professor,
Electrical and Computer Engineering

Suresh K. Khator, Associate Dean,
Cullen College of Engineering

Roberto Ballarini, Professor and Chair,
Civil and Environmental Engineering

ACKNOWLEDGEMENTS

This study would not have been possible without the valuable assistance of several individuals. First, I would like to express my sincere gratitude to my advisor Dr. C. Vipulanandan for providing valuable guidance and encouragement throughout my study. I also would like to thank Dr. Yi-Lung Mo and Dr. Yuhua Chen for serving in my thesis committee.

I wish to acknowledge the past and present members of the GEM group for their support and companionship throughout my research.

Finally, I acknowledge the financial support provided by the CIGMAT, THC-IT, and Jimmie A. Schindewolf Academic scholarship at the University of Houston.

MODIFICATION OF EXPANSIVE SOIL AND REPAIR OF DAMAGED SMART CEMENT USING POLYMER

An Abstract

Of a

Thesis

Presented to

the Faculty of the Department of Civil and Environmental Engineering

University of Houston

In Partial Fulfillment

Of the Requirements for the Degree

Master of Science

in Civil Engineering

by

Mythili Thevamaran

May 2017

ABSTRACT

In this study, acrylamide polymer was used to modify the expansive clays and repair the damaged smart cement. Also the effect of salt contamination on the smart cement behavior was investigated.

In the expansive clay treatment study, index properties, swell potential and swell pressure were quantified to characterize the effectiveness of the polymer treatment. Clay soil with liquid limit in the range of 70-80 % was studied. The addition of 0.3 % of polymer by the weight of dry soil reduced the plasticity index by 35 %.

Failed smart cement specimens were repaired using the acrylamide polymer to recover the piezo-resistivity and the tensile strength. The treatment showed 56-59 % and 71-95 % of recovery in piezo-resistivity at failure peak stress and tensile strength.

Additionally, the tensile piezo-resistive behavior of salt contaminated oil well cement slurry was investigated under splitting tensile loading. Cement composites having sea salt at 2, 4, and 10 % by weight of water, and conductive fillers of 0.1% of total weight of the cement composite were used. While 2 and 4 % of salt contaminated samples did not affect the sensitivity significantly, the 10 % of salt contaminated sample affected the sensitivity adversely.

TABLE OF CONTENTS

LIST OF FIGURES

LIST OF TABLES

CHAPTER 1 INTRODUCTION

This thesis contains three main research investigations: (i) rapid stabilization of expansive soils using polymer, (ii) the tensile piezo-resistive behavior of smart cement with varying conductive filler content and salt content, and (iii) polymer-energy treatment of cracks in damaged smart cement.

1.1 Problem statement

1.1.1 Stabilization of expansive soil

Vulnerability of expansive soils due to moisture changes is a major issue in Geotechnical Engineering. The illite, kaolinite, and montmorillonite are three most prominent clay minerals, which are present in expansive soils. Montmorillonite is more vulnerable to moisture variation than other two minerals (Gromko et al., 1974). Since expansive soils are prone to large volume changes with its moisture variation, it causes damage to buildings, roads, pipelines, and other structures. The estimated annual cost of damage due to expansive soils in United States alone was $15 billion (Buhler et al., 2007).

There are various methods to stabilize the expansive soils such as chemical and mechanical stabilization. Treating the soil with lime and cement changes the pH of the soil up to 13 which affects the biological organisms, increases the urban water runoff, and affects the growth of vegetation. Considering environmental concerns, environment-friendliness, and sustainability, biopolymers and synthetic polymers have been introduced as an alternative to traditional soil treatment, especially for treating expansive soil. There are various polymers widely used for soil treatment such as polyacrylamide, lignosulfonates, acrylics, and phenolasts. Polyacrylamide is appropriate for soil treatment

since its nontoxic and hydrophilic. Anionic polyacrylamide reduces soil erosion and controls the surface runoff (Chang et al., 2016).

Researchers have used various polymers to stabilize the expansive soils (Mirzababaei et al., 2008, Yazdandoust et al., 2010, Azzam et al., 2010, Liu et al., 2011, Naeini et al., 2011, Mohammad et al., 2013, Mousavi et al., 2013). None of them treats the soil rapidly and it takes a minimum of 16 hours to stabilize the expansive soils. Studies about treating expansive soil with polyacrylamide to modify its index properties and swell properties have not been reported yet. So finding a method and its detailed investigation on rapid stabilization of expansive soils with polyacrylamide is absolutely important.

1.1.2 Tensile behavior of Smart cement

The tensile strength, the flexural strength and the compressive strength are important parameters in the design of concrete structures. When appearance, performance, and durability of a structure are considered, tensile strength is an important parameter. Concrete has very low tensile strength compared to its compressive strength (Oluokun et al., 1991). Because of this nature, tensile cracks occur rapidly which is making concrete a brittle material. Even though tensile strength is not considered to be of any significant value in most of the reinforced concrete structural designs, tensile strength plays an important role in the design of mass concrete structures such as dam. When structures are subjected to vibrations or seismic loads, dynamic tensile stresses develop in these structures. For instance, when designing bridges, runways, and pavements, tensile strength is more important than compressive strength (Zain et al., 2002).

Oil well cementing is used to provide zonal isolation between borehole and casing, and it also acts as a seal for gas or any liquid leakages. Oil wells are highly prone to vibrations and seismic load. Therefore, exploring the tensile behavior of oil well cement is crucial for understanding oil well behavior.

Low salt concentration accelerates the hydration of oil well cement and high salt concentration retards it (Zhou et.al, 1996). Salt contamination in offshore structures causes structural failures due to corrosion and deterioration of strength. Absorption of salt by cement slurries modifies its rheology, free fluid and compressive strength (Simao et al., 2012). Salt is used as an accelerator in cold formations (Teodoriu et al., 2015).

There are a few studies about salt contamination based on compressive behavior of cement and concrete (Zhou et al., 1996, Maslehuddin et al., 1996, Simao et al., 2012, Teodoriu et al., 2015). Due to the limited studies in tensile behavior of salt-contaminated oil-well cement, it requires detailed investigations to ensure structural integrity of oil-wells under tensile loadings.

Structural health monitoring is important for structures to ensure its durability and service life time. Monitoring electrical resistivity change in a material due to mechanical stress/strain (Piezo-resistivity) is a technique that can be used in any structure to monitor the structural health throughout its lifetime (Vipulanandan et al., 2014). This technique can be used to investigate tensile behavior of oil well cement and monitor its long term stability. The annual cement production in the world is 4300 million tons in 2017 (ibef.org) which is six times more than the production of rice or wheat. Improving the properties of cement will make a huge impact in the world.

1.1.3 Repair of damaged smart cement

Concrete pipes are used for gravity flow or drainage which provide low stresses. Concrete pipe lines transport materials such as water and oil. Even though concrete pipes are used in low stress level applications, crack occurs in the cementitious material due to shrinkage, temperature variation and mechanical loading. Cracks and leakages are the major causes for most of the structural failures. Repair of such cracks are important to avoid structural failures.

Cementitious structures have self-healing behavior under various circumstances. For instance, micro-crack appeared in a bridge in Amsterdam and was self-healed by the recrystallization of calcite. The reaction between calcium ions and dissolved carbon dioxide attributed to self-healing (Qian et al., 2009).

There are other techniques to repair the cracks in cementitious structures such as using hollow glass fibers carrying air-curing chemicals (Li et al., 1998), electrodeposition method (Ryu et al., 2002), Epoxy and polymethyl methacrylate (Kan et al., 2008), additives like blast furnace slag and limestone powder (Qian et al., 2009) and shrinkable polymers (Jefferson et al., 2010). However, most of the crack repair techniques cannot be used after a structure is constructed. Accessibility to reach the area to be repaired is another issue. Such techniques take quite a long time to repair the cracks. Concerning the factors mentioned, it is important to research a technique that can be used to repair the cracks in cementitious structures.

1.2 Objectives

The overall objective of the study is to stabilize expansive soil and repair of damaged smart cement using acrylamide polymer. The specific objectives are as follows:

1) Develop and characterize the rapid polymer stabilization on expansive soils in terms of its index properties and swelling properties
2) Investigate and characterize the tensile piezo resistive behavior of smart cement and salt contaminated smart cement
3) Develop the polymer-energy method to repair the damage in smart cement and characterize the effectiveness of the technique with its recovery in piezo-resistivity and tensile strength
4) Modeling the behavior of smart cement

1.3 Organization

This thesis is organized into seven Chapters. Chapter 1 explains the introduction of the study which focuses on problem statement. Chapter 2 summarizes literature review of the previous studies done by researchers which is relevant to my research area of interest. In Chapter 3, materials and methods, relevant theories, models and equations used for the research are discussed in detail. The geotechnical behavior of polymer treated expansive soil is presented in Chapter 4. Tensile piezo-resistive behavior of smart cement and salt-contaminated smart cement is discussed in Chapter 5. The repair of damaged smart cement using polymer-energy treatment is discussed in Chapter 6. Finally, major findings of the study and recommendations are summarized in Chapter 7.

CHAPTER 2 BACKGROUND AND LITERATURE REVIEW

2.1 Expansive soil treatment

Previous studies done for expansive soil treatment is summarized in Table 2-1. Various polymers have been used such as Furan (C_4H_4O), Poly methyl methacrylate $(C_5O_0H_8)_n$, Poly vinyl acetate $(C_2H_4O)_x$, Urea Formaldehyde $(OCNCH_2)_n$, Melamine Formaldehyde ($C_4H_8N_6O$), Polypropylene $(C_3H_6)_n$, Acetic-ethylene-ester polymer, Acrylic polymer ($CH_2CRCOOH$), Acrylamide Polymer ($CH_2CHCONH_2$) and Road packer plus polymer. Polymer amount varied from 0.02-18 % of dry soil weight. The types of soil were used are CL and CH. Dry soil was used to treat with the polymer. Standard compaction was used to prepare the samples for unconfined compressive strength, swell potential and swell pressure tests. None of the methods stabilize the soil rapidly and it has taken minimum of 16 hours and maximum of 14 days of curing at room temperature.

Table 2-1 Stabilization of expansive soils with polymers

Reference	Soil type & Location	Sample preparation	Polymer (%)	Curing time	Temperature	Parameters studied	Remarks
Mirzababaei et al., (2008)	CH Location: Iran (0-3 ft)	Standard compaction Dry density: 1.4 g/cm^3 OMC: 33% LL & PI: NA	Furan (3, 5, 10%) PMMA-Poly methyl methacrylate (1, 3, 5%) PVA-Poly vinyl acetate (1, 3, 5%)	2 days	Room	Reduction in Free Swell: Furan 66 % PVA 26 %	Treatment moisture: Dry soil (0 %) Curing time: 2 days Polymer: Furan(10 %)-water insoluble, PVA (5 %)-water soluble
Yazdandoust et al., (2010)	CH Location: Iran	Standard Compaction Density & MC: NA LL (%): 65 PI (%): 41	Urea Formaldehyde (3, 5 % of dry soil wt) Melamine Formaldehyde (5% of dry soil wt)	16 hours	22℃ for swelling, 40℃ for shrinkage	Reduction in Swell potential: 82 % Swell pressure: 62 %	Treatment moisture: Dry soil (0 %) Curing time: 16 hours Polymer: 5 %, water soluble
Azzam et al., (2010)	CH Location: Egypt (0-2.5 ft)	Standard Compaction Bulk Density: 1.74 g/cm^3 OMC: 13% LL & PI: NA	polypropylene (5, 10, 15 % of dry soil wt)	NA	80℃ for shrinkage	Reduction in PI: 43 % Free Swell : 67 % Swell Pressure: 71 %	Treatment moisture: Dry soil (0 %) Curing time: NA Polymer: 15 %, water insoluble

NA: Not Available, LL: Liquid limit, PL: Plastic limit, OMC: Optimum moisture content, UCS: Unconfined compressive strength

Table 2-1 Stabilization of expansive soils with polymers (continued)

Reference	Soil type & Location	Sample preparation	Polymer (%)	Curing time	Temperature	Parameters studied	Remarks
Liu et al., (2011)	CH Location: China	Standard compaction Bulk Density: 1.71 g/cm^3 OMC: 15% LL (%):52.6 PI (%): 19.7	acetic-ethylene-ester polymer (17.8% of dry soil wt)	3 days	25℃	Increase in UCS : 272 %	Treatment moisture: Dry soil (0 %) Curing time: 1 day Polymer: 17.8 %, water soluble
Naeini et al., (2011)	CL, CH Location: Iran	Modified Proctor compaction (ASTM D-1557) Dry density: 1.92-1.84 g/cm^3 OMC: 12-14% LL (%):31-52 PI (%): 12-26	Acrylic polymer (maximum of 5% of optimum water content wt)	8 days	21-25℃	Increase in UCS: CL: 163 % CH: 154 %	Treatment moisture: Dry soil (0 %) Curing time: 8 days Polymer: 4 %, water soluble

NA: Not Available, LL: Liquid limit, PL: Plastic limit, OMC: Optimum moisture content, UCS: Unconfined compressive strength

Table 2-1 Stabilization of expansive soils with polymers (continued)

Reference	Soil type & Location	Sample preparation	Polymer (%)	Curing time	Temperature	Parameters studied	Remarks
Mohammed et al., (2013)	CL Location: Field	Standard compaction Dry density: 1.88 g/cm^3 OMC: 10% LL (%):23 PI (%): 9	Acrylamide Polymer (0-15% of dry soil wt)	1 day	Room	Increase in UCS: 760 %	Treatment moisture: Dry soil (0 %) Curing time: 1 day Polymer: 10 %, water soluble
Mousavi et al., (2013)	CH Location: Iran	Standard compaction Dry density: 1.34 g/cm^3 OMC: 27% LL: 89 % PI (%): 54	Road packer plus polymer (0.019, 0.04, 0.06% of dry soil wt)	7, 14 days	Room	Reduction in LL: 15 % PI: 19 % Swell Potential: 57 % Swell pressure: 90 %	Treatment moisture: Dry soil (0 %) Curing time: 14 days Polymer: 0.06 %, water soluble
Remarks	CL, CH Field soil was used	Mainly Standard compaction Dry density: 1.34-1.92 g/cm^3 OMC: 10-33% LL: 23-65 % PI: 9-41 %	Various polymers maximum of 18%	16 hours - 14 days of curing	Room temperature	Reduction in PI- 43 %, Swell potential-82 %, Swell pressure-90 %	Dry Clay was treated with 0.06-18 % of water soluble polymers. Minimum of 16 hours of curing. Reduction in index properties and swell properties.

NA: Not Available, LL: Liquid limit, PL: Plastic limit, OMC: Optimum moisture content, UCS: Unconfined compressive strength

2.2 Smart cement and piezo-resistivity

The placement of oil well cement between the casing of oil well and surrounding rock is called oil well cementing and this process is challenging since it is done far below to the ground and deals with high pressure and temperature. The primary goal of oil well cementing is to restrict fluid movement between formations and to bond and support the casing.

Xie (1996) studied about effect of conductive fiber content in cement composites containing carbon fiber and steel fiber. According to their study, the composite conductivity depends only in fiber content. When fiber content reaches a threshold value, conductivity is changed by several orders of magnitude. So it is important to find the minimum fiber content to produce conductive composite.

Carbon fibers are used as conductive fillers in cement. Since carbon fibers are electrically conductive, there is change in electrical resistance when the smart cement undergoes stress or strain (Wang et al., 1998).

Even though carbon fibers are relatively expensive than other fibers such as glass fibers, basalt fibers and plastic fibers, due to its unique properties such as conductive, light weight, high chemical resistance, high temperature tolerance, high stiffness and high tensile strength, it is popular among research industries. Sim (2005) studied about carbon fibers, basalt fibers and glass fibers and reported that when carbon fibers are immersed in alkali (1 M NaOH) solution for 28 days, no reaction between carbon fibers and alkali solution was observed and there was no significant reductions in volume (<20%) and tensile strength (<13%) as well, whereas basalt and glass fibers reacted with alkali solution

and lost their volumes and strength significantly. Carbon fiber was stable even under weathering test such as ultra-violet exposure. Under thermal stability test, carbon fiber was stable up to 200℃.

The conductive behavior of carbon fibers is used to modify the electrical resistivity in cement composites based on the various applications. Vipulanandan (2008) studied about electrical resistivity and mechanical properties of carbon fiber rein-forced cement mortar. In this study, the specific electrical resistivity of plain mortar with w/c ratio of 1 was reduced from >66,000 Ωm to 3,750 and 0.23 Ωm by adding carbon fibers of 1-6% of total weight of the composite. They reported that increasing the carbon fiber content increased the peak strain and toughness, but decreased the Young's modulus and electrical resistivity of cement mortar composites.

Piezo-resistivity is defined as a change in electrical resistivity of a material due to mechanical stress or strain (Vipulanandan et al., 2014). There is no monitoring technique currently available in the oil well construction industries to monitor the fresh cement and hardened cement during its lifetime. Smart cement, cement modified with conductive filler, is having better sensing properties which can be monitored throughout the life time of oil wells (Vipulanandan et al., 2014).

2.3 Splitting tension

In general, tensile strength of a cementitious material is measured by direct tension test, flexural test and splitting tensile test. In comparison with other methods, splitting tensile test is simple and produces a reliable result (Choi et al., 2005). Splitting tensile strength can be related to compressive strength, water binder ratio and concrete age and strength development pattern of splitting tensile strength and compressive strength are similar (Zain, et al., 2002). In general, splitting tensile strength is greater than direct tensile strength and lower than flexural strength and it is used to design lightweight cementitious members (ASTM C496).

Splitting tensile tests done by researchers from previous studies have been summarized in Table 2-2. Most of the studies had focused on the splitting tensile strength of concrete made of Portland cement reinforced with fibers such as carbon fiber, carbon steel fiber, glass fiber, calcium carbonate whisker, polypropylene fiber, and basalt fiber. The minimum of 0.1 % and a maximum of 10 % of fiber content by weight of cement had been used for the tensile studies. In general, specimens were cured for 28 days at room temperature and 100 % of humidity. Splitting tensile strength of concrete varied from 2.2 to 5.5 MPa and results showed a maximum of 62 % of increment in splitting tensile strength due to fiber addition. Particularly, a maximum of 0.3 % of carbon fibers by weight of cement had increased the tensile strength by 41 %.

Table 2-2 Splitting tensile test with various types of fibers

Reference	Materials	Mechanical Testing	Fiber type & amount (%)	Curing Conditions	Split tensile (MPa)	Remarks
Wafa et al., (1992)	Ordinary Portland cement, Aggregates	Split tensile, Compression, Flexural strength	Carbon steel fiber: 0-1.5% (Vol)	Curing time: 28 days (under water) Temperature: 25˚C Humidity: 100%	Change: from 6.45-10.04	55% increment due to Carbon steel fiber
Siddique et al., (2003)	Ordinary Portland cement, Aggregates, Fly ash (0-50 % of fine aggregates)	Split tensile, Compression, Flexural strength	–	Curing time: 28 days Temperature: 26-28˚C Humidity: Not available	Change: from 3-3.5	16% increment due to Fly ash
Choi et al., (2005)	Ordinary Portland cement, Aggregates	Split tensile, Compression	Glass fiber: 0-1.5 % (Vol), Polypropylene Fiber: 0-1.5 % (Vol)	Curing time: 28 days Temperature: 25˚C Humidity: 100%	Change: GF: from 2.23-3.06 PF: from 2.23-3.21	37% increment due to Glass fiber, 44% increment due to Polypropylene fiber

Table 2-2 Splitting tensile strength with various types of fibers (continued)

Reference	Materials	Mechanical Testing	Fiber type & amount (%)	Curing Conditions	Split tensile (MPa)	Remarks
Dias et al., (2005)	High early strength Portland cement (PC), Geopolymeric cement (GC), Aggregates	Split tensile, Compression, Flexural strength	Basalt fiber: 0-1% (Vol)	Curing time: 28 days Temperature: Not available Humidity: 100%	Change: PC: from 2.5-2.2 GC: from 3.2-4.0	PC: 12% decrement due to Basalt fiber, GC: 25% increment due to Basalt fiber
Ming et al., (2015)	Class G oil well cement	Split tensile, Compression, Flexural strength	Carbon fiber (CF) : 0-0.3 % of Cement wt, Calcium carbonate whisker (CW): 0-10 % of cement wt	Curing time: 28 days Temperature: 30˚C Humidity: Not available	Change: CF: from 3.35-4.75 CW: from 3.40-4.10 Hybrid: from 3.40-5.50	41% increment due to Carbon fiber, 20% increment due to Calcium carbonate whisker, 62% increment due to hybrid fibers
Remarks	Portland cement was used in general	Split tensile, Compression, Flexural strength were done	Minimum of 0.1 % and Maximum of 10 % of fibers by weight of cement	In general, Curing time- 28 days Mostly room temperature Humidity 100% was used	Minimum of 2.2 MPa and Maximum of 5.5 MPa have been reported	0.3 % of Carbon Fibers by weight of cement have increased the tensile strength by 41 %. Range of tensile strength- 2.2-5.5 MPa.

2.4 Salt contamination in oil well cement

Low salt concentration accelerates the hydration of oil-well cement while high salt concentration retards it (Zhou et al., 1996). Absorption of salt by cement slurries modifies its rheology, free fluid, and compressive strength (Simao et al., 2012). Salt water is used to mix oil-well cement due to its abundance and ready availability in off shore construction (Teodoriu et al., 2015). Even after the construction, salt water seepages into offshore structures. Salt contamination in oil-well cement slurries has both good and adverse effects in its fresh properties and hardened properties. These effects depend on the salt concentration in the contaminated cement slurry, temperature, and pressure. Salt is used to accelerate the hydration of cement slurry when pumping in cold formations (Teodoriu et al., 2015). According to Teodoriu (2015), positive effects on setting time, rheology, strength, and hydraulic integrity occurred for low salt contamination, but there are some adverse effects such as increment in permeability have occurred due to high salt concentration in oil-well cement.

There have been studies about compressive behavior of salt contaminated oil well cement whereas tensile behavior of salt contaminated oil well cement has not been reported yet. As summarized in Table 2-3, Class G cement was used as oil well cement. The Salt content varied from 0-37 % by the weight of water. Up to 5 % of salt content had increased the strength by 38-41 % while more than 5 % of salt content had decreased the strength by 26-69 %. The salt content up to 37 % by the weight of water did not change the density of the slurry.

Table 2-3 Compressive behavior of salt contaminated cementitious materials

Reference	Materials	Mechanical Testing	Salt type & amount (%)	Curing time	Temperature/ Pressure	Compressive strength (MPa)	Remarks
Zhou et al., (1996)	Class G cement	Compression test	NaCl table salt: 0-36 % BWOW	72 hrs	93 °C / 20.7 MPa 160 °C / 20.7 MPa	0 %: 50 5 %: 48 36 %: 28 0 %: 32 5 %: 27 36 %: 17	5 % of salt: 4 % reduction in compressive strength 36 % of salt: 44-47 % reduction in compressive strength Density: NA
Maslehuddin et al., (1996)	Ordinary Portland cement V, 3% of CO_2 exposure	Compression test	NaCl: 0-0.8 %	54 weeks	55 °C RH 75 %	0 %: 32 0.8 %: 26	0.8 % of salt: 19 % reduction in compressive strength Density: NA
Simao et al., (2012)	Class G cement	Compression test	NaCl: 0-36 % BWOW	8 hrs 7 days	60 °C 60 °C	0 %: 13 5 %: 18 36 %: 4 0 %: 29 5 %: 27 36 %: 12	5 % of salt: 38 % increase in compressive strength 36 % of salt: 59-69 % reduction in compressive strength Density: NA

BWOW: By the weight of water, NA: Not Available

Table 2-3 Compressive behavior of salt contaminated cementitious materials (continued)

Reference	Materials	Mechanical Testing	Salt type & amount (%)	Curing time	Temperature/ Pressure	Compressive strength (MPa)	Remarks
Teodoriu et al., (2015)	Class G cement	Compression test	NaCl:0-37 % BWOW	1, 3, 7 days	18.5 °C / 1 bar 30 °C / 100 bar	0 %: 27 5 %: 38 37 %: 20 0 %: 44 5 %: 48 37 %: 25	5 % of salt: 41 % increase in compressive strength 37 % of salt: 26-43 % reduction in compressive strength Density: no change
Remarks	Class G cement was used in general	Compression test was done	NaCl 0-37 % BWOW was used	7 days in general	18-160 °C	Range: 0 %: 13-50 5 %: 18-48 37 %: 4-28	Up to 5 % of NaCl has increased the compressive strength by 38-41 %. More than 5 % of NaCl has decreased the strength by 26-69 %. NaCl content did not change the density.

BWOW: By the weight of water, NA: Not Available

2.5 Crack repair

The structural stability and durability of cementitious structures are compromised due to the cracks in the structures. There is various crack closure mechanisms reported in the literatures.

Jacobson (1996) reported about self-healing of high strength concrete after deterioration by freeze/thaw. The damaged specimens were stored in water for 2-3 months and their resonance frequency, weight, volume and compressive strength were compared to see the effectiveness of the self-healing. Dynamic modulus was recovered completely and compressive strength recovered 4-5 % due to self-healing.

Li (1998) demonstrated about a passive smart self-healing cementitious composite in which superglue, Ethyl cyanoaacrylate, serves as the sealing chemical contained in hollow brittle glass fibers. The elastic modulus was found to regain its original value due to self-healing of the composite.

Ryu (2002) reported that reinforced concrete beams damaged by chloride attack were healed by electrodeposition method in which specimens were immersed in ZnSO4 solution and applied a constant current for 8 weeks. The electrodeposits formed during this process were able to close the cracks and reduced the permeability.

Concrete cracks were repaired using epoxy mortar and polymethyl methacrylate (PMMA) mortar. The results revealed that concrete with a flexural crack has a higher restoring efficiency than that with a shearing crack when repaired with epoxy mortar and PMMA mortar. Increasing the amount of sand inclusion in the mortar increases the restoring efficiency (Kan et al., 2008).

Qian (2009) investigated self-healing behavior of strain hardening cementitious composites incorporating blast furnace slag and limestone powder with relatively higher water/binder ratio. He reported the deflection capacity of beams recovered about 65-105 % from virgin specimens due to the continuous hydration of cementitious materials.

Conventional pre- and post-tensioned structures are generally designed to be uncracked under serviceability loading. (Jefferson et al., 2010). Jefferson (2010) studied the crack closure system for cementitious materials using shrinkable polyethelene terephthalate polymer tendons. Crack closure was achieved by thermally activating the shrinkage mechanism of the restrained polymer tendons after the cement based material had undergone initial curing.

Zanotti (2017) investigated the bond strength of Portland cement concrete specimens and geopolymer (alkali-activated metakaolin-based repair mortar). The early-age cracking was prevented with mild heat curing at 45 °C for 24 hours. Heating accelerated the geopolymer reaction as well. The repair took 28 days and improved the shear bond strength and crack growth resistance. The heat cured repaired specimens showed higher compressive strength (47.8 MPa) compared to ambient cured repaired specimens (31.3 MPa).

2.6 Summary

From the literature review of the studies of expansive soil treatment, tensile piezo-resistive behavior of smart cement and salt-contaminated smart cement, and repair of damaged cementitious materials, following can be concluded.

1) The dry expansive soils have been stabilized with various polymers and the polymer amount varied from 0.02-18 % of dry soil weight. None of the methods stabilize the soil rapidly and it has taken minimum of 16 hours and maximum of 14 days of curing at room temperature.
2) The minimum of 0.1 % and a maximum of 10 % of fiber content by weight of cement had been used for the tensile studies. Split tensile strength of concrete varied from 2.2-5.5 MPa. A maximum of 0.3 % of carbon fibers by weight of cement had increased the tensile strength by 41 %. None of the studies had reported about tensile piezo-resistivity.
3) While compressive behavior of salt contaminated oil well cement had been reported, tensile behavior of salt contaminated oil well cement has not been reported yet. Up to 5 % of salt content had improved the compressive strength by 38-41 % and more than 5 % of salt content had decreased the strength by 26-69 %.
4) The duration reported in literature for various crack repair techniques of damaged cementitious materials varied from 8 weeks- 3 months. The recovery of compressive strength was 4-5 % while elastic modulus regained completely.

CHAPTER 3 MATERIALS AND TESTING METHODS

3.1 Polymer stabilization of expansive soil

The materials used for the stabilization of expansive clay and the testing methods used for the characterization of the untreated and treated soils were discussed in this section.

3.1.1 Clay

Commercially available clays Kaolinite and Na-Bentonite, shown in Figure 3-1 (a) and (b), were used for this study. The Kaolinite and Na-Bentonite mainly have kaolinite and montmorillonite minerals respectively and their chemical composition is summarized in Table 3-1. The specific surface area of Kaolinite and Na-Bentonite are 30-46 m^2/g and 600-800 m^2/g respectively (Sigma Aldrich-MSDS).

(a)

(b)

Figure 3-1 Clays (a) Kaolinite and (b) Bentonite

Table 3-1 Clay composition (webmineral.com)

Clay minerals	Chemical composition
Kaolinite	$Al_2Si_2O_5(OH)_4$
Montmorillonite	$(Na,Ca)_{0.33}(Al,Mg)_2(Si_4O_{10})(OH)_2 \cdot nH_2O$

3.1.2 Acrylamide polymer

Polyacrylamide gel (AV100) is made with copolymerization of acrylamide and bis-acrylamide. Polymerization is initiated by ammonium persulfate (AV102) and activated by triethanolamine (AV101). Chemical composition of the components of the polymer are summarized in Table 3-2.

Table 3-2 Chemical composition of Polyacrylamide polymer (Inyang et al., 2007)

Title	**Chemical composition**
Acrylamide	C_3H_5NO
Ammonium persulfate	$(NH_4)_2S_2O_8$
Triethanolamine	$C_6H_{15}NO_3$

Solution A was prepared with 1 g of AV100, 1 g of AV101, and 48 g of water. Solution B was prepared with 10 g of AV102 and 40 g of water as summarized in the Table 3-3. A 15 g of solution A and a 15 g of solution B were used to treat the synthetic clay separately to see the effect of the solutions alone. Then, solutions A and B were mixed together and then from the 100 g of polymer solution, only a 30 g of polymer solution was

used to treat the 100 g of dry synthetic clay. So the amount of acrylamide used to treat the soil was 0.3 % of dry soil weight.

Table 3-3 Solution A and Solution B for synthetic clay treatment

Solution A	**Solution B**
AV 100- 1 g	AV 102- 10 g
AV 101- 1 g	Distilled water- 40 g
Distilled water- 48 g	

To treat the natural expansive soil, solution A and B were prepared as summarized in Table 3-4. A 10 g of polymer solution was used to treat the 100g of solid content of natural soil.

Table 3-4 Solution A and Solution B for natural expansive soil treatment

Solution A	**Solution B**
AV 100- 3 g	AV 102- 15 g
AV 101- 1 g	Distilled water- 35 g
Distilled water- 46 g	

3.1.3 Liquid limit test (ASTM D4318)

The moisture content that defines where the soil changes from plastic to viscous fluid state is called liquid limit. According the ASTM D4318 standard, the moisture content at 25 blows is considered as liquid limit.

Synthetic clay mix was mixed with 30 g of polymer solution thoroughly. Once polymer coated almost all the soil particles, distilled water was added to do the liquid limit test. Liquid limit test was done for both untreated and polymer treated soils. Four sets of readings were taken for each test to increase the accuracy. Figure 3-2 shows the device and other tools used for this test.

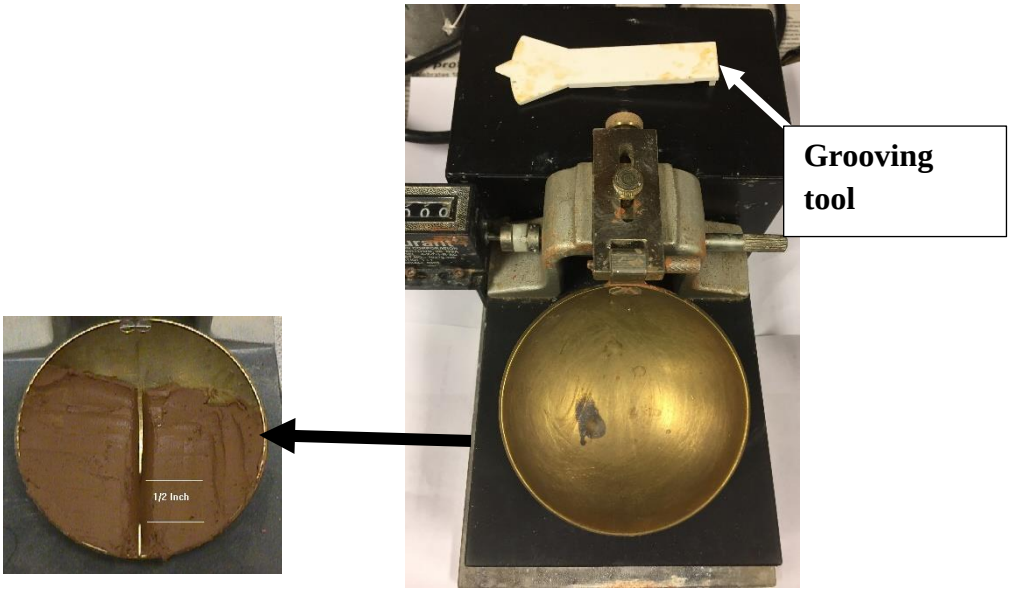

Figure 3-2 Liquid limit test device: Cassagrande cup method

3.1.4 Plastic Limit test

The moisture content that defines where the soil changes from plastic to semisolid state is called plastic limit. At plastic limit, soil will start to crumble when rolled into a thread of 3 mm diameter in a flat surface as shown in Figure 3-3. Plastic limit test was done for the untreated and polymer treated soil mix. Three sets of reading were taken for each test.

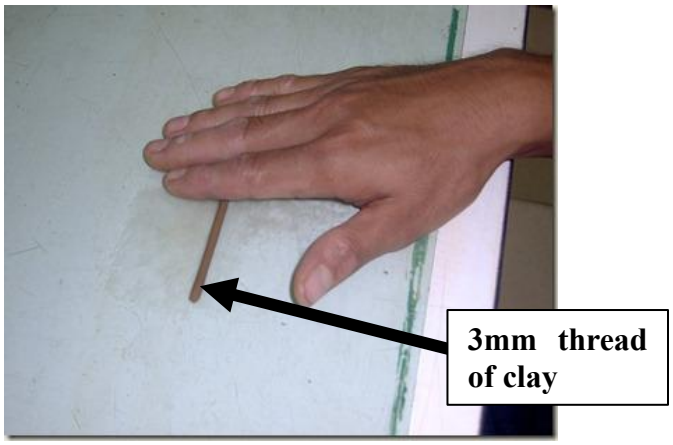

Figure 3-3 Plastic limit test

3.1.5 Standard proctor compaction test (ASTM D680)

Dry clay with 95 % of Kaolinite and 5 % of Bentonite was mixed and then distilled water was added to maintain 20-25 % of initial moisture content. Soil mixture was kept in an air tight plastic bag for 24 hours. Then the soil mixture was compacted in 3 layers with 25 blows per layer. Hammer weight was 2.5 kg and drop height was 300 mm. Figure 3-4 shows the hammer and mold which were used for this test.

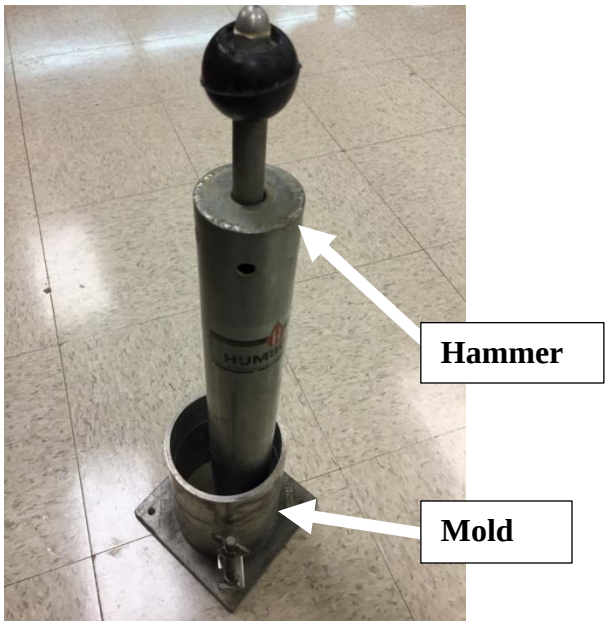

Figure 3-4 Standard proctor compaction test apparatus

3.1.6 Swell potential of soils (ASTM D4546)

Swell potential of a soil is one dimensional swelling of a soil, which is 100 times the difference between final and initial height of the specimen divided by the initial height. The classification of swell potential of soils was summerized in Table 3-5. As mentioned in standard compaction test, soil mixture was compacted to get required dry density. The greased consolidation ring was used to cut the soil sample and with spatula, sample was leveled at the top and bottom for swell potential test. Leftover soil was used to get the initial moisture content. As shown in the Figure 3-5, sample was set in an oedometer apparatus. Distilled water was used to inundate the sample. Vertical pressure of 1 psi (6.9 kPa) was applied during the test. Deformation of the soil was recorded until it reached the rate of deformation 0.0002 in/h.

Table 3-5 Classification of swell potential of soils (ASTM D4829)

Swell potential	Potential expansion
0-2	Very low
2.1-5	Low
5.1-9	Medium
9.1-13	High
>13	Very high

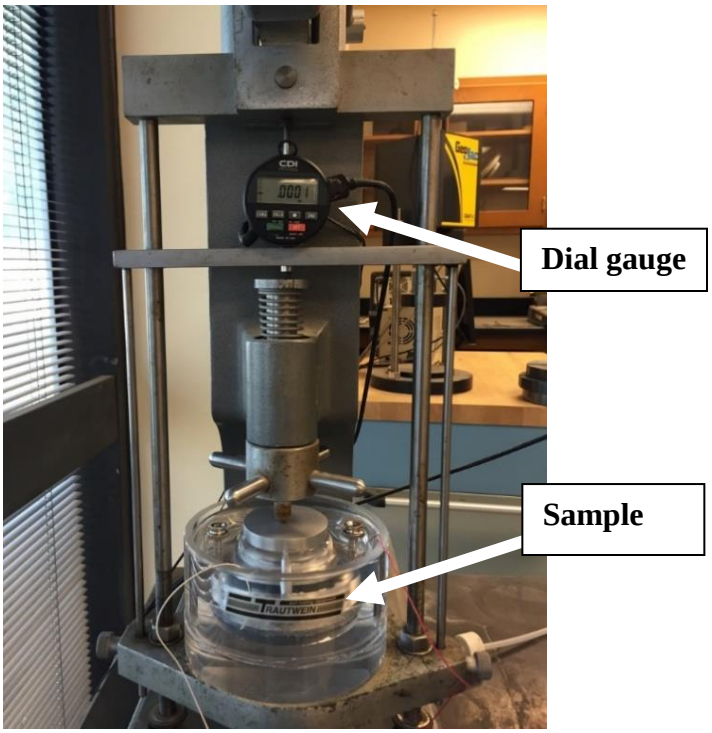

Figure 3-5 Oedometer apparatus

3.1.7 Swell pressure test

The soil sample was prepared as mentioned in the swell potential test in section 3.1.6 and it was allowed to swell at its maximum under the vertical pressure of 1 psi. Once it's swelled completely, the vertical pressure was increased in increments until the sample was compressed to its initial height prior to swell as shown in the Figure 3-6. So the total pressure used to compress the sample to its initial height was considered as swell pressure. This procedure is called the loading after swell method.

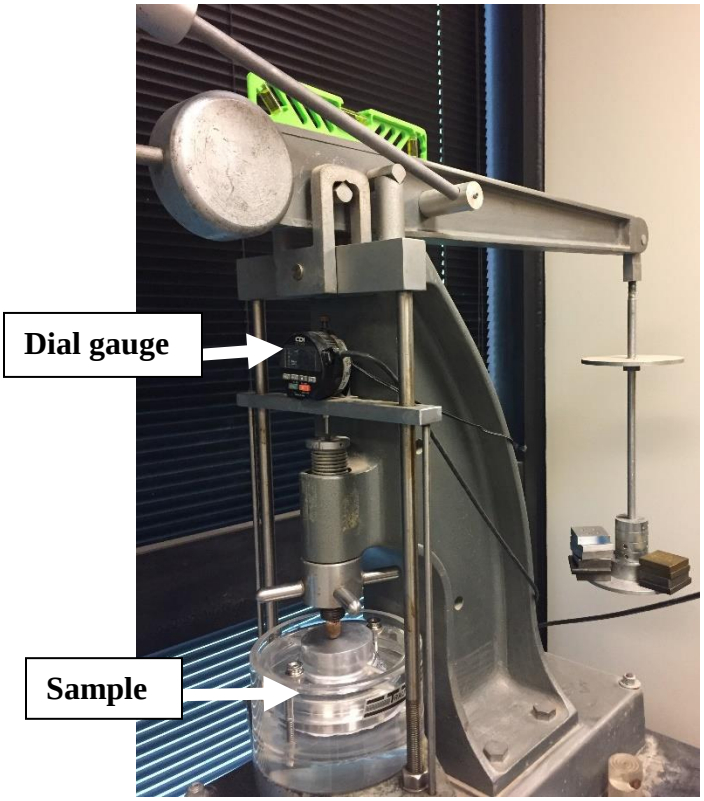

Figure 3-6 Swell pressure test

3.2 Tensile piezo-resistive behavior

3.2.1 Smart cement

The API RP 10B-2 standard was adapted for the preparation of smart cement specimens. Class H cement was used as a binder. Conductive fillers content was varied from 0.05-0.15% of total weight. Water to cement ratio was 0.38. Cylindrical molds were used with the height of 4 inches and the diameter of 2 inches. As shown in Figure 3-7, there are four probes embedded in the mold to measure the piezo-resistivity in both longitudinal and lateral directions to the specimen. Cement specimens were demolded after 24 hours of curing and cured at room temperature for 28 days. Splitting tensile test was done after 28 days. The loading rate was 0.01 in/min.

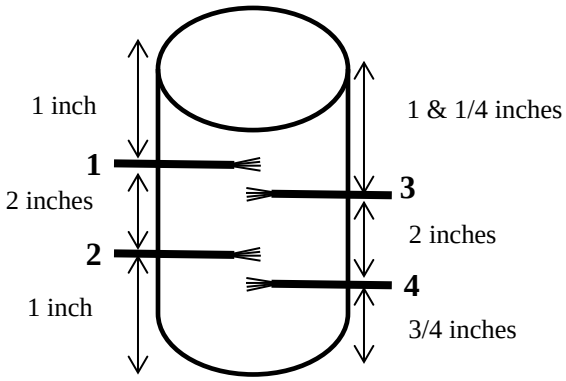

Figure 3-7 Schematic diagram of specimen configuration

3.2.2 Salt contaminated smart cement

Sea salt of 2%, 4% and 10 % of weight of water were mixed with water first and then mixed with class H cement and conductive fillers of 0.1% of total weight of cement composite. As mentioned in section 3.2.1, specimens were prepared and cured for 28 days

and then split test was done. Resistivity and resistance were measured for fresh cement slurry and resistance measurements were continued until the split test is done.

3.2.3 Electrical Resistivity

API resistivity meter and conductivity meter were used to measure initial resistivity of the fresh smart cement slurry before it starts setting. Measuring initial resistivity assures the homogeneity of the mix. LCR device is used to measure the initial resistance of the smart cement slurry. Resistance was used to find the K-factor, shown in equation 3-1,

$$R = \frac{\rho * L}{A} = \rho * K, \qquad 3\text{-}1$$

where R is Electrical resistance, ρ is Electrical resistivity, L is Length between electrodes, A is Cross sectional area, and K is Geometric factor. The K-factor was used to calculate the cement resistivity once it's hardened. Curing was monitored in terms of resistivity for a day.

3.2.4 Piezo-resistivity

Piezo-resistivity is defined as a change in electrical resistivity of a material due to mechanical stress/strain. LCR was used to measure the resistance of the smart cement when tensile mechanical stress is applied. Measurements of resistance and stress were taken until the failure of the specimen.

The equation 3-2,

$$\frac{\Delta\rho}{\rho} = \frac{\Delta R}{R}, \qquad 3\text{-}2$$

was used to quantify electrical resistivity change with respect to electrical resistance change.

3.2.5 Impedance

Equivalent circuits were proposed in literature (Vipulanandan et al., 2013) to represent piezo resistive cementitious materials. In Figure 3-8, probes (contacts) are represented by a resistor and a capacitor in parallel, bulk material is represented by a resistor, and both contacts are connected to the bulk in series connection.

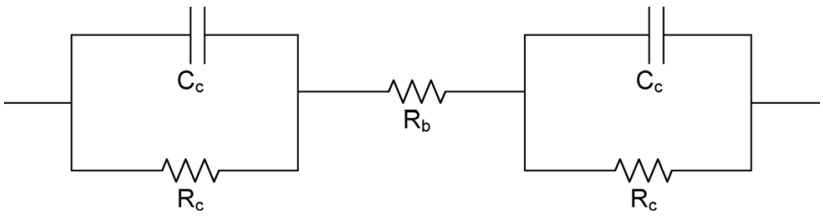

Figure 3-8 Equivalent circuit for case 2

Here R_c is contact resistance, C_c is contact capacitance, and R_b is bulk resistance.

Impedance of the above equivalent circuit is given by

$$Z = R_b + \frac{2*R_c}{1+\omega^2*R_c^2*C_c^2} - j * \frac{2*\omega*R_c^2*C_c}{1+\omega^2*R_c^2*C_c^2} \quad . \qquad 3\text{-}6$$

When the frequency of the applied signal is very low, $\omega \rightarrow 0$, $Z = R_b + 2R_c$ and when the frequency is very high, $\omega \rightarrow \infty$, $Z = R_b$.

3.2.6 Split tensile test

The Splitting tensile strength (indirect tensile strength) test as shown in Figure 3-9 was carried out according to ASTM C 496. The peak load at the first crack was used to calculate the splitting tensile strength. Splitting tensile strength can be expressed as

$$f_t = \frac{2*P}{\pi*D*L}, \qquad 3\text{-}3$$

where f_t is splitting tensile strength, P is applied load, D is diameter of the specimen, L is length of the specimen.

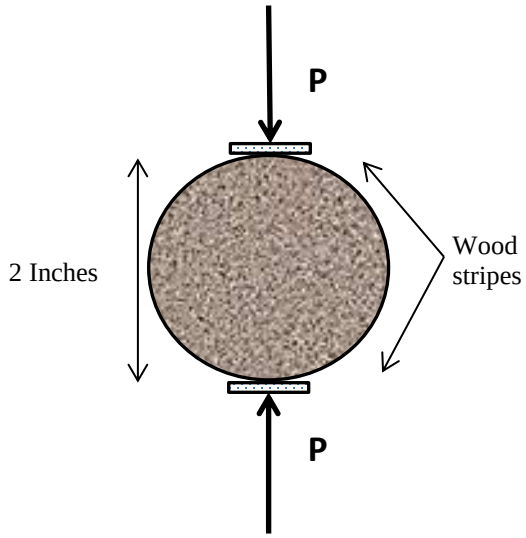

Figure 3-9 Schematic diagram of split tensile test

Smart cement is assumed to be an isotropic and elastic material and the failure under the state of stress is represented by the principle stresses σ_1,

$$\sigma_1 = \frac{6*P}{\pi*D*L} \ , \qquad 3\text{-}4$$

$\sigma_2 = 0$ and σ_3,

$$\sigma_3 = -\frac{2*P}{\pi*D*L} \ . \qquad 3\text{-}5$$

The first invariant of the stress tensor, I_1,

$$I_1 = \sigma_1 + \sigma_2 + \sigma_3 \quad . \qquad 3\text{-}6$$

The second invariant of the deviatoric stress tensor, J2,

$$J_2 = \sqrt{\left\{\frac{1}{6}\left[(\sigma_1 - \sigma_2)^2 + (\sigma_2 - \sigma_3)^2 + (\sigma_3 - \sigma_1)^2\right] + \tau_{12}^2 + \tau_{23}^2 + \tau_{31}^2\right\}} \ . \qquad 3\text{-}7$$

The first invariant of the stress tensor, I_1 and second invariant of the deviatoric stress tensor, J_2 were correlated in this study.

3.2.7 Direct tensile test

Smart cement slurry was prepared as mentioned in section 3.2.1. The amount of conductive filler content was 0.1 % of total weight of the specimen. Dog-bone shape mold was used to cast the specimen. Specimen was cured at 100 % of humidity to avoid drying shrinkage. Extensometer was used to measure the strain in the direction of the stress as shown Figure 3-10. Displacement measurements were taken from the automated load test system as well. LCR was used to measure the resistance during the load was applied.

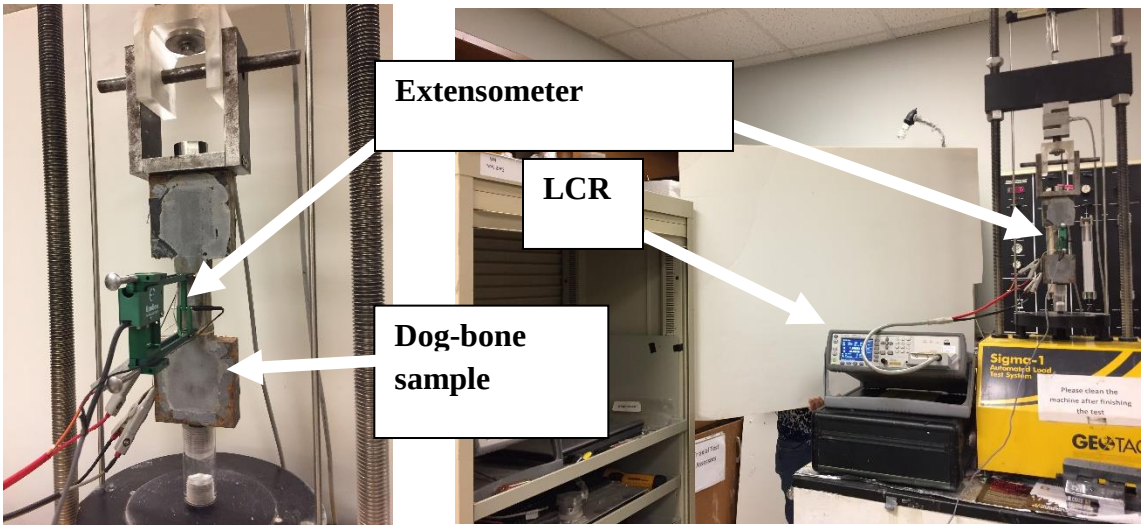

Figure 3-10 Experimental setup for direct tensile test

3.3 Polymer-Energy treatment of tensile crack

Hollow cylindrical smart cement specimens were made for this study. As mentioned in the section 3.2.1, smart cement slurry was made with conductive filler content of 0.1 %. As shown in the Figure 3-11, greased cylindrical and solid pipes made of Teflon were used to create hollow in the specimens. Specimens were cured under water for 28 days to avoid shrinkage cracks. Split test was done after 28 days of curing. Tensile strength and piezo-resistivity were calculated from the load and resistance data to characterize the initial state of the specimens before repair.

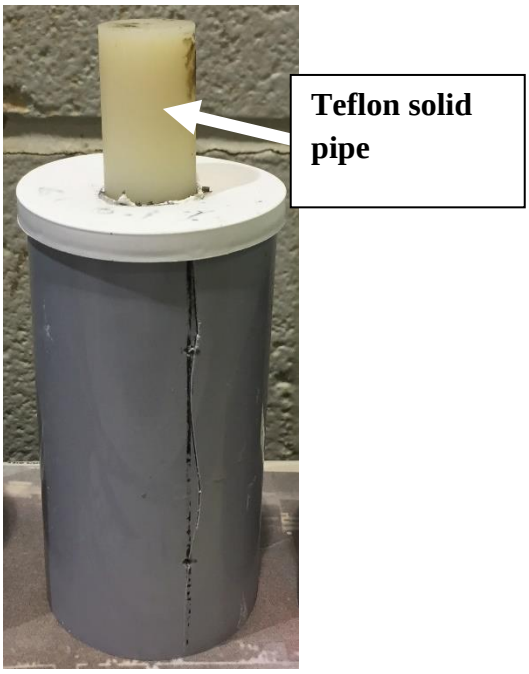

Figure 3-11 Mold for hollow specimen

In addition to the hollow specimens, the failed specimens from the studies of tensile piezo-resistive behavior of smart cement and salt contaminated smart cement were also used for this study.

Acrylamide polymer was used as a repair material which had a setting time of 5 minutes. The damaged specimen was kept inside the High Temperature High Pressure (HTHP) cylindrical chamber. Solution A and B were prepared as mentioned in Table 3-6 and poured into the HTHP chamber. Then, a pressure of 150 psi was applied to pressurize the polymer solution into the cracks of the damaged specimen for 5 hours. After the pressurizing process, the specimen was immersed in polymer solution and connected with DC supply as shown in the Figure 3-12(a) and (b) to supply a current of 0.01 A for 7 days. Weight and resistance measurements were taken during the process of polymer-energy treatment. After 7 days of treatment, split test was done to quantify the recovered piezo-resistivity and tensile strength.

The Joule's law is

$$Q = I^2 \times R \times t, \qquad 3\text{-}4$$

where Q is total energy, I is electrical current, R is resistance, and t is time. It was used to calculate the total energy supplied during the treatment

Table 3-6 Solution A and Solution B of polymer-energy treatment

Solution A	**Solution B**
AV 100- 7.4-8 g	AV 102- 2 g
AV 101- 4 g	Distilled water- 98 g
Distilled water- 88-88.6 g	

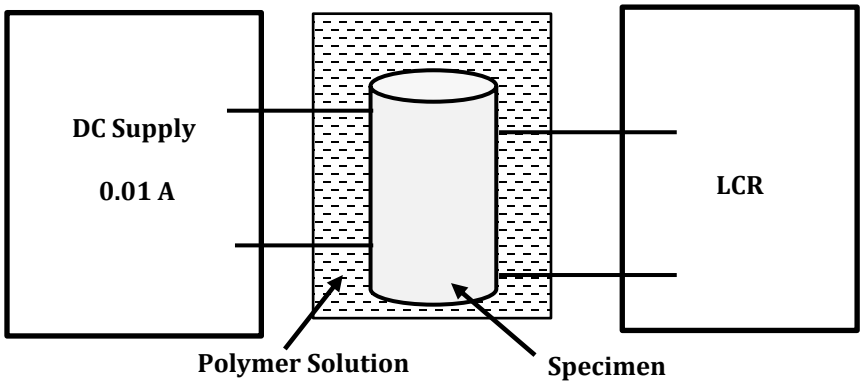

(a)

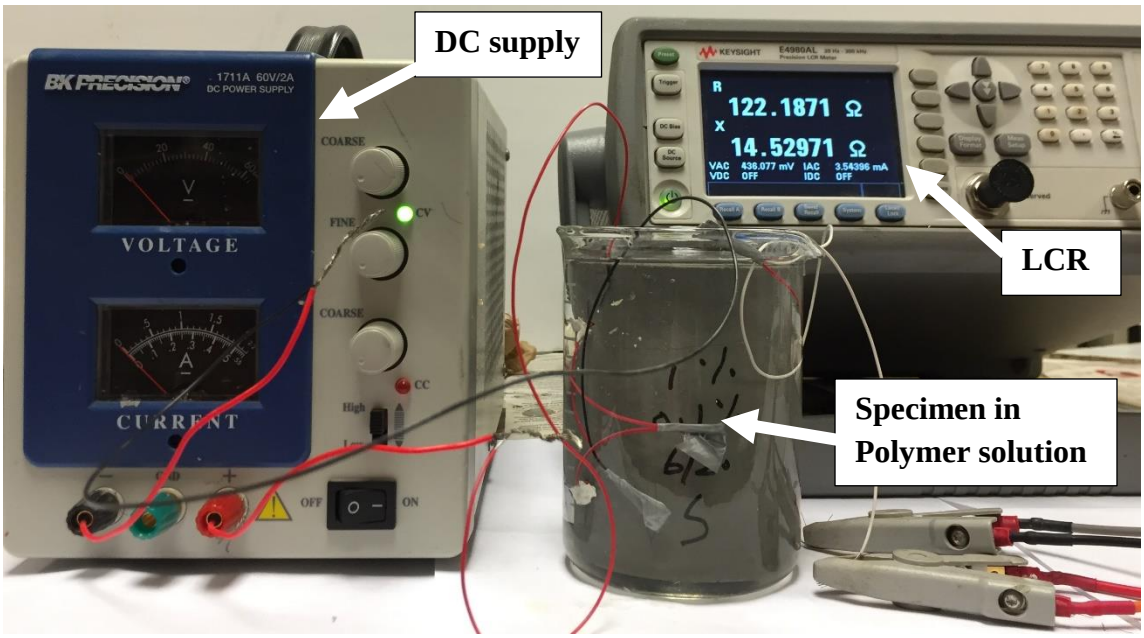

(b)

Figure 3-12 (a) Schematic diagram of crack treatment (b) Actual setup

3.4 Devices used for the studies

3.4.1 LCR meter

LCR meter (Inductance Capacitance Resistance meter), shown in Figure 3-13, was used to measure initial resistance and the resistance change during the splitting tensile test. This can measure resistance with a varying frequency from 20 Hz to 300 kHz. In this study, a higher frequency of 300 kHz was chosen for the consideration of bulk resistance. The applied voltage was 1 volt and alternating current was used to eliminate electrolysis of oil well cement slurry and polarization of waves.

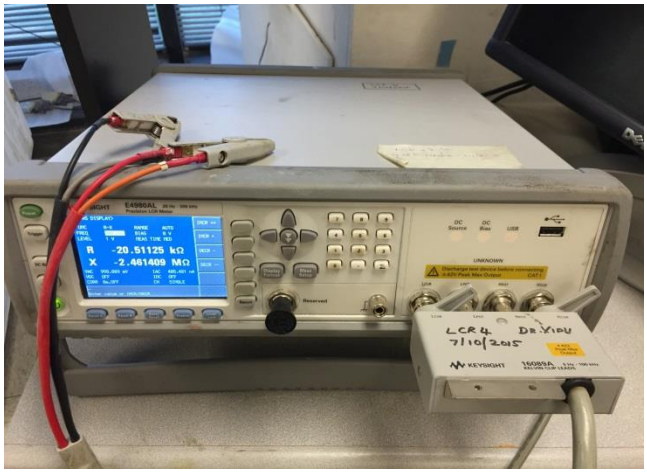

Figure 3-13 Agilent E4980A LCR meter

3.4.2 API resistivity meter

API resistivity meter shown in Figure 3-14 was used to measure electrical resistivity of fresh cement slurry to assure the homogeneity of the mix. This can measure from 0.01 Ωm to 400 Ωm.

Figure 3-14 API resistivity meter

3.4.3 Conductivity meter

The electrical resistivity is the reciprocal of electrical conductivity. Conductivity meter, shown in Figure 3-15, was used to double check the accuracy of the electrical resistivity measurements. It can measure a conductivity range from 0.1 μS/cm to 1000 mS/cm, which is equivalent to a resistivity of 10,000 Ω·m to 0.1 Ω·m.

Figure 3-15 Conductivity meter

3.4.4 DC supply

DC supply, shown in Figure 3-16, was used to supply 0.01 A of current for the polymer-energy treatment of damaged smart cement specimens. This device can supply a maximum of 30 V.

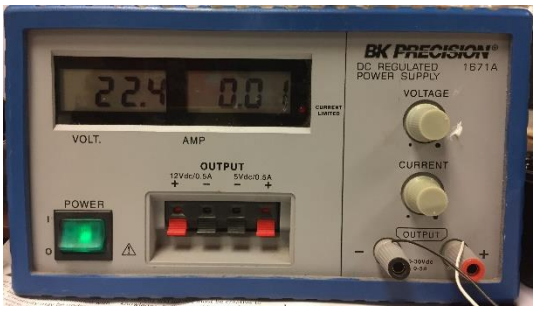

Figure 3-16 DC supply

3.4.5 High Temperature High Pressure Device (HTHP)

HTHP, shown in Figure 3-17, was used to pressurize (150 psi) the polymer solution into the cracks of damaged smart cement specimens.

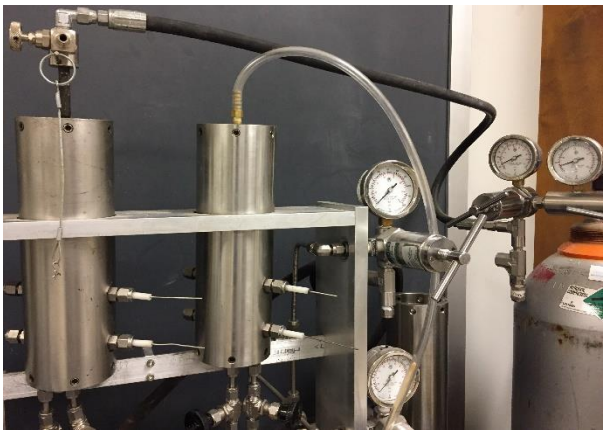

Figure 3-17 HTHP Device

3.5 Modeling

3.5.1 Electrical resistivity modeling

The p-q model was proposed by Vipulanandan and Paul (1990) to represent compressive stress-strain behavior of epoxy mortar. In this study, p-q model was used to represent the electrical resistivity variation of smart cement and salt contaminated smart cement while curing for a day. The relationship is as follows:

$$\frac{1}{\rho} = \frac{1}{\rho_{min}} * \left[\frac{\frac{t+t_0}{t_{min}}}{q_1+(1-p_1-q_1)*\left(\frac{t+t_0}{t_{min}}\right)+p_1*\left(\frac{t+t_0}{t_{min}}\right)^{\frac{q_1+p_1}{p_1}}} \right] . \qquad 3\text{-}4$$

This model was used to predict the results where p_1 and q_1 are material parameters, ρ_{min} is the minimum resistivity during hydration of smart cement, and the t_{min} is the time to reach the minimum resistivity.

3.5.2 Piezo-resistivity modeling

In this study, p-q model was used to represent the tensile piezo-resistive behavior of oil well cement. The relationship is as follow:

$$\sigma = \frac{\sigma_{max}*\left(\frac{\left(\frac{\Delta\rho}{\rho}\right)}{\left(\frac{\Delta\rho}{\rho}\right)_0}\right)}{q_2+(1-p_2-q_2)*\left(\frac{\left(\frac{\Delta\rho}{\rho}\right)}{\left(\frac{\Delta\rho}{\rho}\right)_0}\right)+p_2*\left(\frac{\left(\frac{\Delta\rho}{\rho}\right)}{\left(\frac{\Delta\rho}{\rho}\right)_0}\right)^{\left(\frac{p_2+q_2}{p_2}\right)}} . \qquad 3\text{-}5$$

This model was used to predict the results. Here, p_2 and q_2 are material parameters, σ_{max} is maximum stress, $\frac{\Delta\rho}{\rho}$ is change in resistivity.

CHAPTER 4 POLYMER MODIFICATION OF EXPANSIVE SOIL

The stabilization of expansive soil with acrylamide polymer was discussed in this chapter. Synthetic clay was made for the study using commercially available kaolinite and bentonite. Natural soil was used for the study to see the effectiveness of the expansive soil stabilization using polymer in the field. Geotechnical properties of untreated and treated expansive soils such as liquid limit, plastic limit, plasticity index, dry density, expansion index and swell pressure were compared to characterize the stabilization of expansive soil with polymer.

4.1 Selection of synthetic expansive soil

Commercially available kaolinite and bentonite were mixed to create expansive soil. The Cassagrande cup method was used to measure the liquid limit of synthetic soil mix. The linear mixture theory equation was expressed as

$$LL = X * LL_1 + (1 - X) * LL_2, \qquad 4\text{-}1$$

where LL is liquid limit of the mix, LL_1 is liquid limit of kaolinite, LL_2 is liquid limit of bentonite, and X is the percentage of kaolinite. The equation 4-1 was used to calculate the liquid limit in terms of the proportions of various soil types and their corresponding liquid limits. This calculation was done to check the linearity of the liquid limit of soil when it was mixed with various types of soil contents. The soil proportions, measured and calculated liquid limits are summarized in the Table 4-1.

Table 4-1 Proportion of kaolinite and bentonite and liquid limit of the mix

Kaolinite	Bentonite	LL(measured)	LL(predicted)
100	0	47±1	47
95	5	76±1	81
90	10	102±2	114
85	15	122±2	148
80	20	143±10	182
0	100	720±20	720

The pure kaolinite and bentonite had 47 % and 720 % of liquid limits respectively as shown in Figure 4-1(a) and (b). Since the liquid limits of natural expansive soils used for this study were in the range of 70-80 %, the synthetic clay mix with 95 % of kaolinite and 5 % of bentonite which had a 76 % of liquid limit, as shown in Figure 4-2, was chosen for further studies.

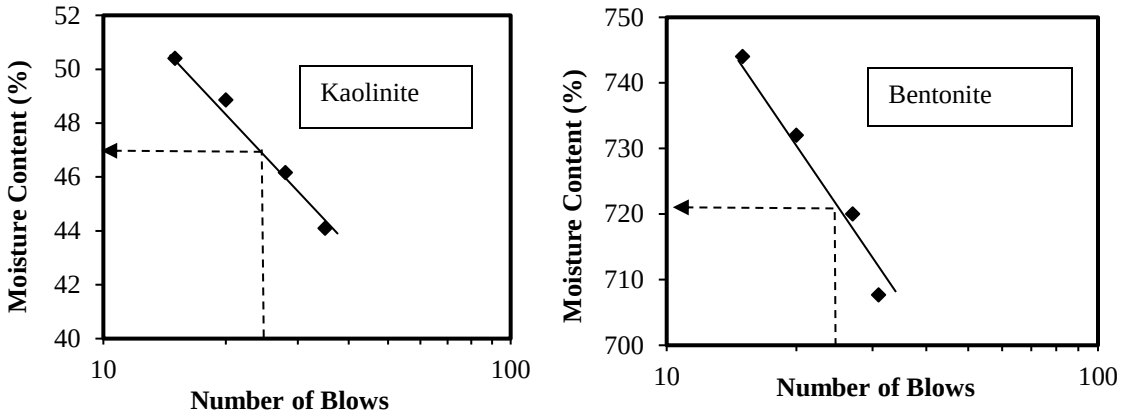

(a) (b)

Figure 4-1 Liquid limit of (a) kaolinite and (b) bentonite

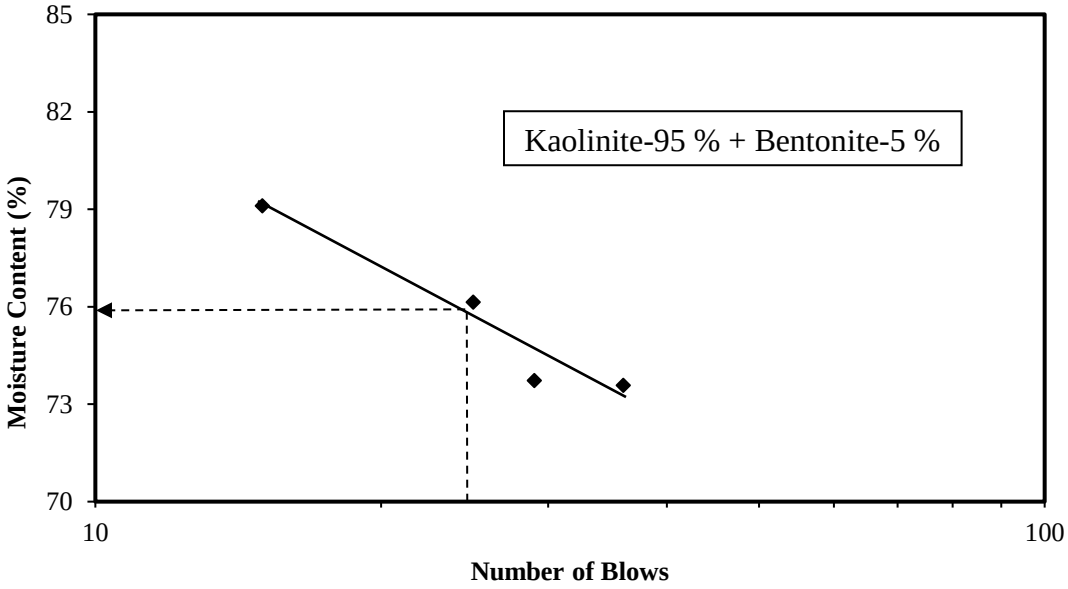

Figure 4-2 Liquid limit of synthetic clay (mix of kaolinite and bentonite)

The liquid limit, plastic limit and plasticity index of kaolinite, bentonite and soil mix with 95 % of kaolinite and 5 % of bentonite are summarized in Table 4-2. The soil mix made for the study can be classified as high plasticity clay (CH) since its liquid limit (76 %) is more than 50 %.

Table 4-2 Summary of Index properties of synthetic clay

Soil type	Liquid limit (%)	Plastic limit (%)	Plasticity Index (%)
Kaolinite	47±1	19±1	28±2
Bentonite	720±20	103±10	617±30
Mix	76±1	29±1	47±2

4.2 Index properties of polymer treated synthetic clay

Acrylamide polymer solution was prepared by combining solution A and solution B as explained in section 3.1.2. The synthetic clay was treated using 15 g of solutions A and 15 g of solution B separately to see the effect of the solutions alone with expansive clay. The obtained results are shown in Figure 4-3 and Figure 4-4. Solution A and B increased the liquid limit from 76 to 82 and from 76 to 79 respectively.

When 30 g of polymer solution (solution A and B combined) was used to treat the expansive clay, it decreased the liquid limit from 76 to 60 as shown in Figure 4-5.

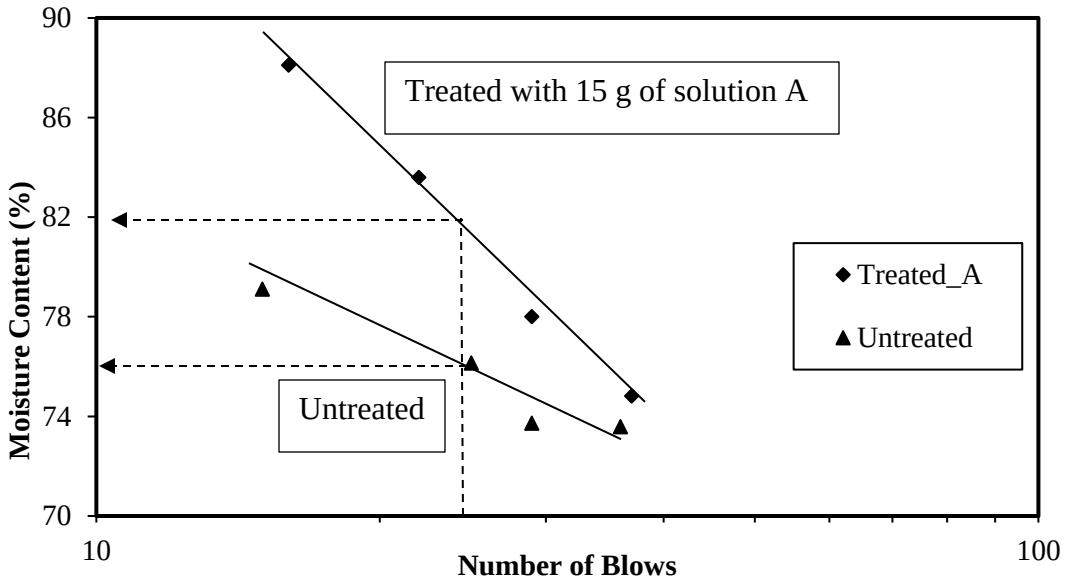

Figure 4-3 Liquid limit of soil when treated only with Solution A

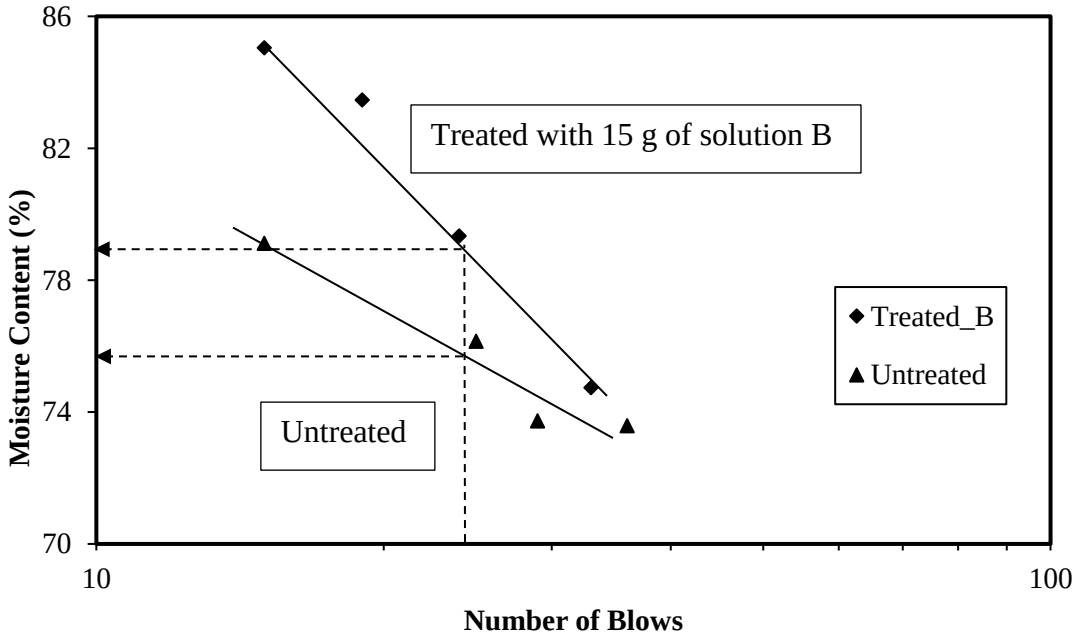

Figure 4-4 Liquid limit of soil when treated only with Solution B

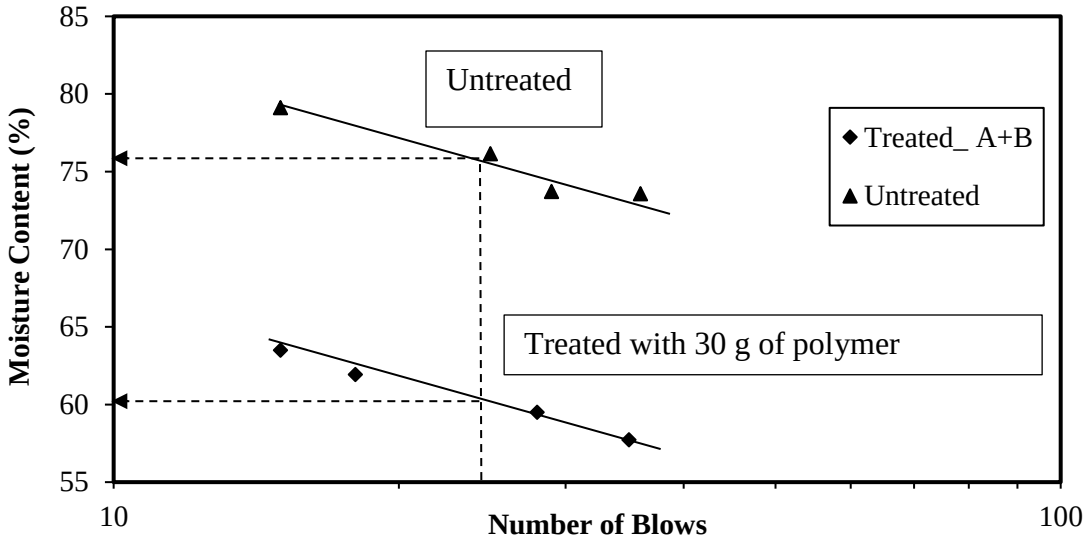

Figure 4-5 Liquid limit of soil when treated with polymer solution (A+B)

The index properties of polymer treated synthetic expansive clay are summarized in Table 4-3. The soils treated with solution A and B separately increased the plasticity index compared to untreated soil. Only the polymer solution, which had solutions A and B combined, decreased the plasticity index from 47 % to 24 %, a 49 % of reduction.

Table 4-3 Index properties of treated synthetic clay

Solution	Liquid limit (%)	Plastic limit (%)	Plasticity Index (%)
Untreated	76±1	29±1	47±2
A	82±1	30±1	52±2
B	79±1	29±1	50±2
A+B	60±1	36±1	24±2

4.3 Swell potential test

Swell potential test was done for untreated and polymer treated soils according to ASTM D 4546. Soil parameters for untreated and treated soils are summarized in Table 4-4. After the standard compaction, untreated soil had 22 % of moisture content. Since a 30 g of polymer solution was used to treat the dry soil, its initial moisture content after standard compaction was 27 % which was 5 % higher than the initial moisture content of untreated soil. While there was a difference of 0.08 g/cm^3 of bulk density, the dry density was same for both untreated and treated soils. It indicated the solid content is same for untreated and treated soils.

Table 4-4 Soil parameters of untreated and polymer-treated soils

Soil Properties	Untreated	Treated
Initial moisture content (%)	22	27
Final moisture content after swelling (%)	41	32
Bulk density (g/cm^3)	1.80	1.88
Dry density (g/cm^3)	1.48	1.48

The swell potential of untreated and polymer treated soils were 23.3 % and 4.7 % as shown in Figure 4-6 and the enlarged version of treated soil was given in Figure 4-7. The untreated soil had taken 70.5 hours to reach its maximum swell potential whereas polymer treated soil had taken 47.7 hours. An 80 % of reduction in swell potential had occurred due to polymer stabilization.

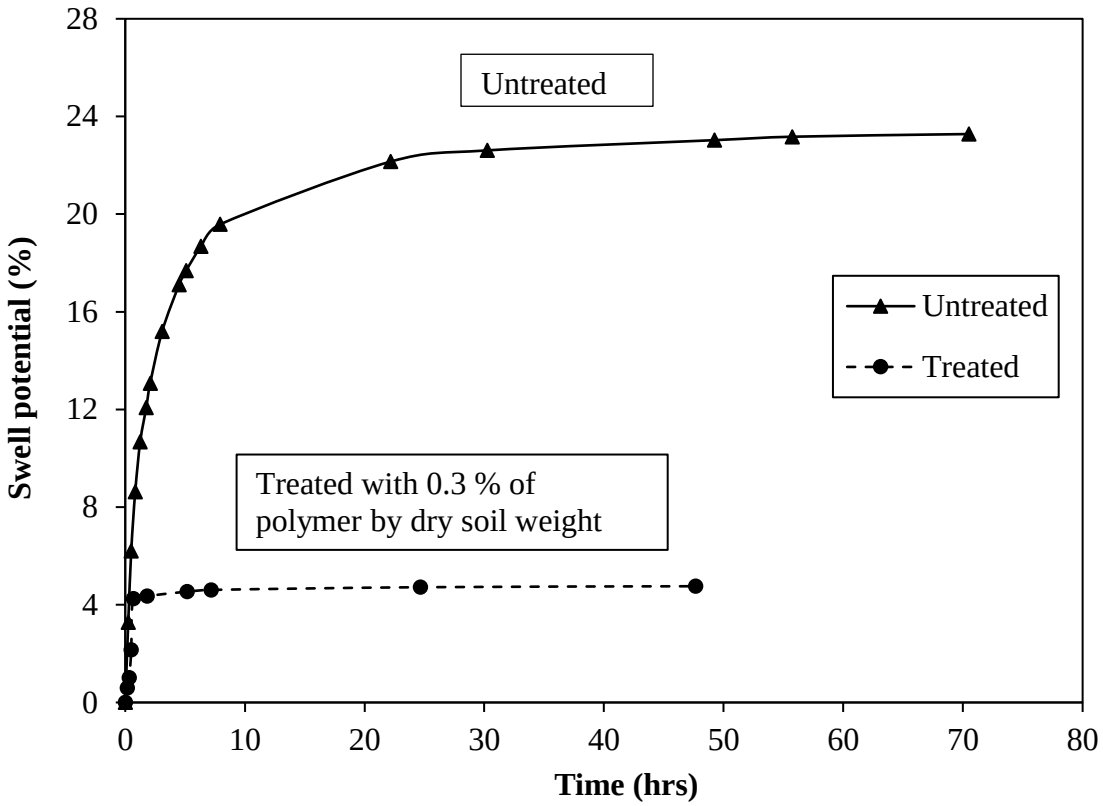

Figure 4-6 Swell potential of untreated and treated soil

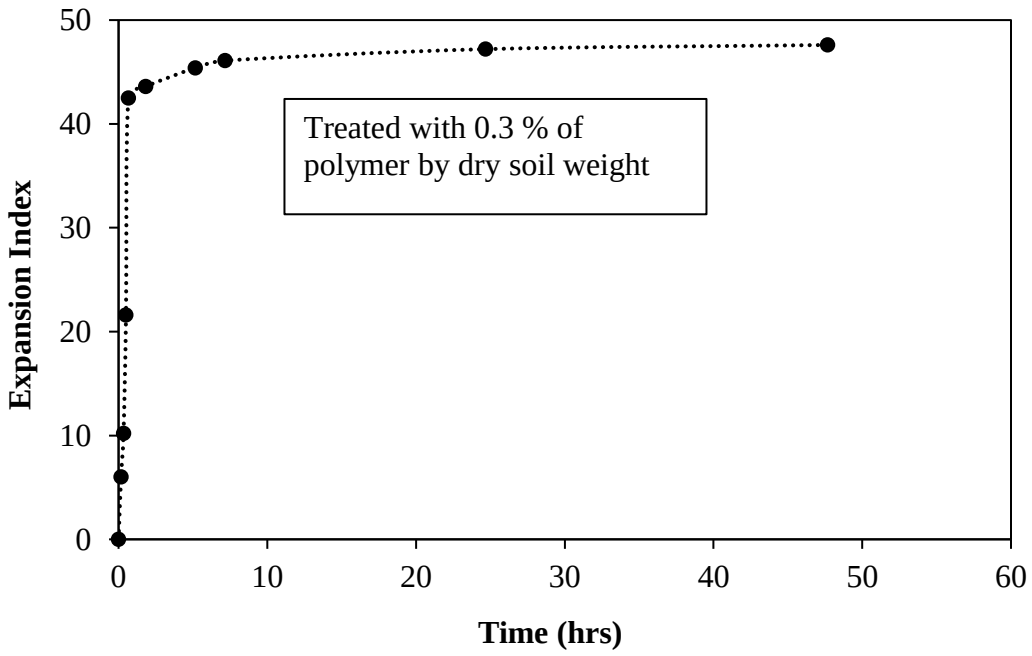

Figure 4-7 Swell potential of polymer treated soil

4.4 Swell pressure test

The swell pressure test was done to characterize the effectiveness of the polymer in expansive soil treatment. The loading after swell method was used to measure the swell pressure of the soil in this study. Once the expansive soil swelled completely, the pressure used to compress the sample to its initial height was considered as swell pressure.

The swell pressure of untreated and treated soils are summarized in Table 4-5. The swell pressure of untreated and polymer treated soils were 19.76 and 15.58 psi respectively. Due to the polymer treatment of the soil, a 21% of reduction had occurred in swell pressure.

Table 4-5 Swell pressure of untreated and treated soils

Soils	Swell pressure (psi)
Untreated	19.76
Polymer treated	15.58

4.5 Acrylamide polymer treatment of natural expansive soil

A borehole sample at 8-10 ft depth from field was used for this study. Soil properties are summarized in Table 4-6. Natural soil was high plasticity clay since it had a 75 % of liquid limit which is more than 50 %. Plasticity index was 43 %.

Table 4-6 Soil properties of field soil

Bulk density (g/cm^3)	2.0
Initial moisture content (%)	28
Liquid limit (%)	75±2
Plastic limit (%)	32±1
Plasticity Index (%)	43±3

When 100 g of solid content from natural soil was treated with the 30 g of polymer (0.3 % of polymer by dry weight of soil), which was the amount used to treat the synthetic clay, it increased the liquid limit from 75 % to 95 %, as shown in

Figure 4-8. When 10 g of polymer solution (0.3 % of polymer by dry weight of soil) was used, the liquid limit decreased from 75 %to 65 %. Since the natural soil already had 28 % of moisture and the polymer solution had more than 29 % of moisture, there was too much of moisture for the treatment and it may decrease the polymer absorption of soil particles. So, polymer concentration was increased by 3 times to reduce the moisture during soil treatment and to optimize the polymer absorption of soil particles.

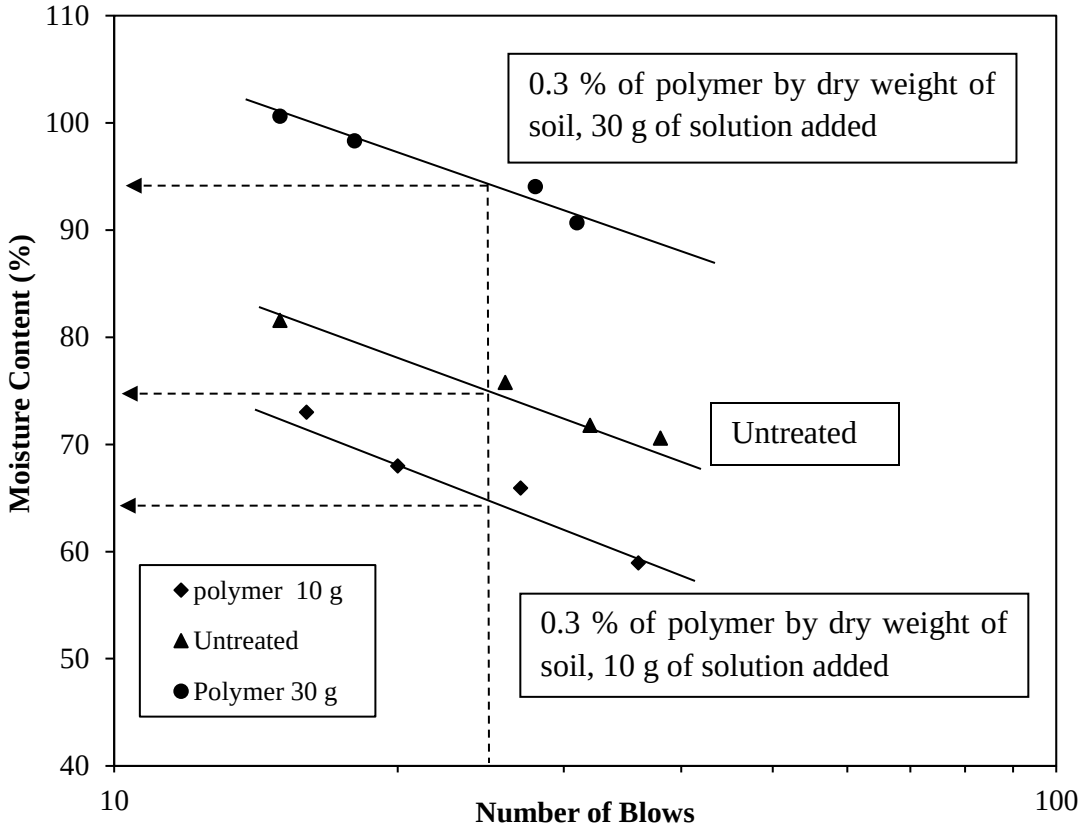

Figure 4-8 Liquid limit for untreated and polymer treated natural soil

The index properties of natural soil before and after polymer treatment are summarized in Table 4-7. The liquid limit and plasticity index reduced by 14 % and 35 % and plastic limit increased by 15 % due to polymer stabilization.

Table 4-7 Index properties of untreated and polymer-treated natural soil

Index properties	**Untreated**	**Polymer treated**
Liquid limit (%)	75±2	65±1
Plastic limit (%)	32±1	37±1
Plasticity index (%)	43±3	28±2

4.6 Classification of polymer treated soil

Plasticity chart was used to represent the classification of untreated and polymer treated fine grained soils as shown in Figure 4-9. U-line in the plasticity chart represents the upper limit of the combination of liquid limit and plasticity index of soils. A-line in the plasticity chart separates the clay soil from silt soil. The untreated soils were classified as high plasticity clay. The treated soils had transformed to high plasticity silt from high plasticity clay due to polymer stabilization.

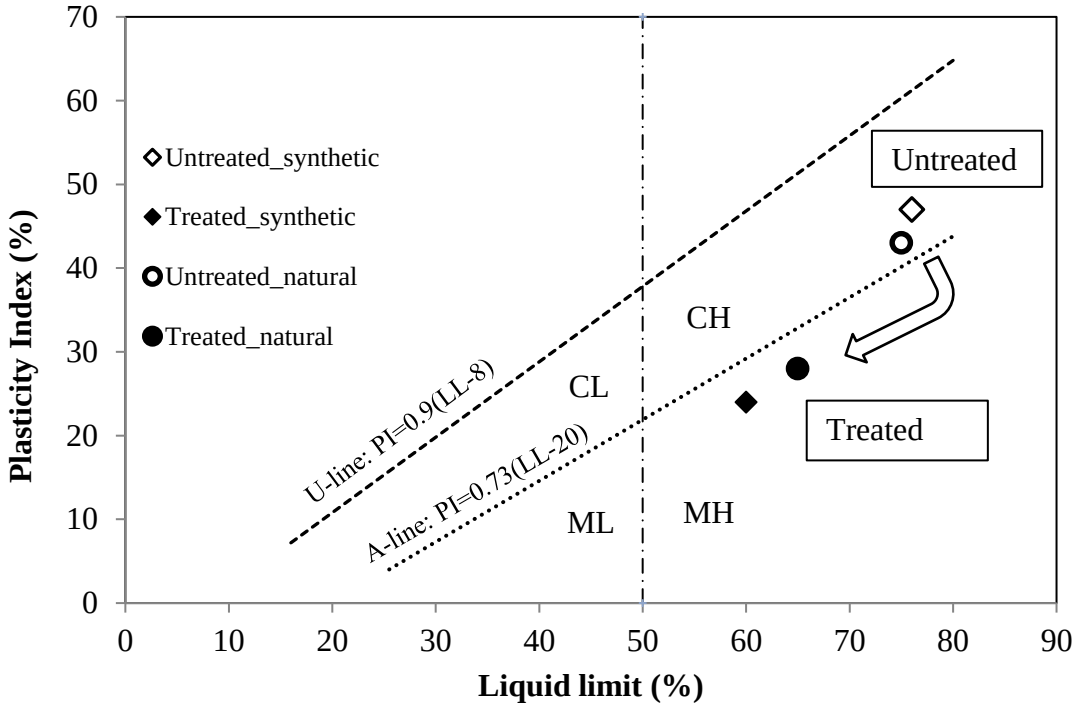

Figure 4-9 Plasticity chart for untreated and polymer treated soils

CH: High plasticity Clay, CL: Low plasticity Clay, MH: High plasticity Silt, ML: Low plasticity Silt

4.7 Summary

The number of tests done for synthetic and natural clays were 15 and 7 respectively. Based on the results obtained for rapid stabilization of synthetic and natural expansive soils using acrylamide polymer, the following can be concluded.

1. An amount of acrylamide polymer 0.3 % of dry soil weight was effective for the rapid stabilization of both synthetic and natural expansive soils.
2. The rapid stabilization of synthetic expansive clay reduced the liquid limit and plasticity index by 21 % and 49 % respectively and increased the plastic limit by 24 %.
3. An 80 % of reduction in swell potential and a 21 % of reduction in swell pressure were obtained for synthetic clay from the swell potential test.
4. The natural clay obtained from field also justified the efficiency of the acrylamide polymer on expansive soil treatment with a 35 % of reduction in its plasticity.
5. Since natural soil already had 28 % of moisture, the amount of polymer solution had to be reduced by increasing its concentration to avoid too much of moisture during treatment. It was observed that polymer absorption of wet soil was less than that of dry soil.
6. The expansive soils had changed from high plasticity clay to high plasticity silt due to acrylamide polymer stabilization.

CHAPTER 5 TENSILE PIEZO-RESISTIVE BEHAVIOR

In this chapter, tensile piezo-resistive behavior of smart cement and salt contaminated smart cement are discussed. Also the variation in density for smart cement slurry with conductive filler contents and salt contents was investigated. The characterization of curing and hydration for a day in terms of resistivity measurements are documented. Direct tensile and split tensile tests were performed to characterize the material. The p-q model was used to model and interpret the hydration of smart cement in terms of electrical resistivity, tensile piezo-resistivity and stress-strain behavior.

5.1 Percolation characterization

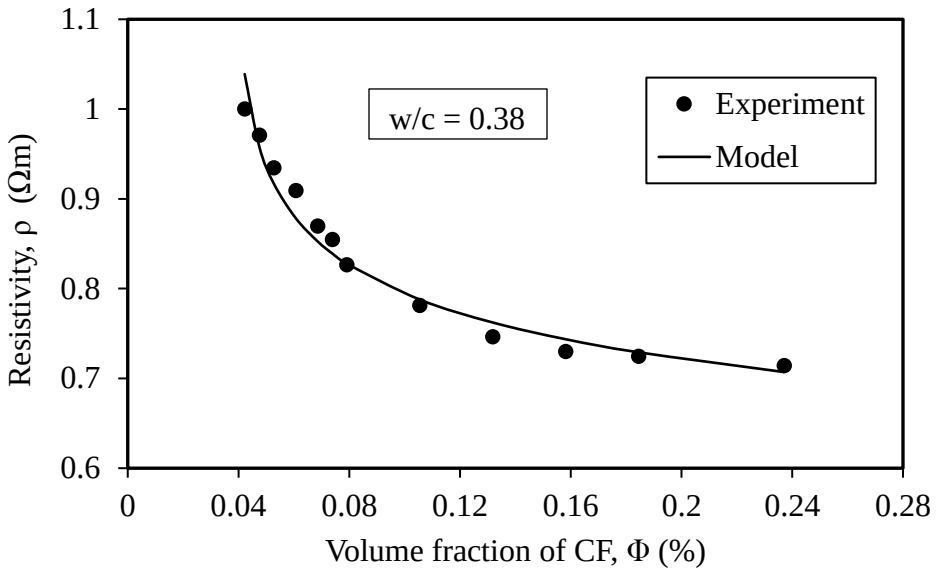

Figure 5-1 Resistivity variation with conductive filler (CF) contents in the cement

The percolation threshold was obtained as shown in Figure 5-1. The equation,

$$\rho_i = A\rho_{fiber} (\phi - \phi_{critical})^{-t_i} \quad , \qquad 5\text{-}1$$

was used to model the percolation characterization. The sudden decrease in resistivity occurred when the volume fraction of the conductive filler content was 0.038 %. The model parameters are summarized in Table 5-1.

Table 5-1 Model parameters

A	t	ϕ Critical	R^2	RMSE (Ωm)
34783	0.099	0.038	0.96	0.02

5.2 Density of smart cement with varying conductive filler contents

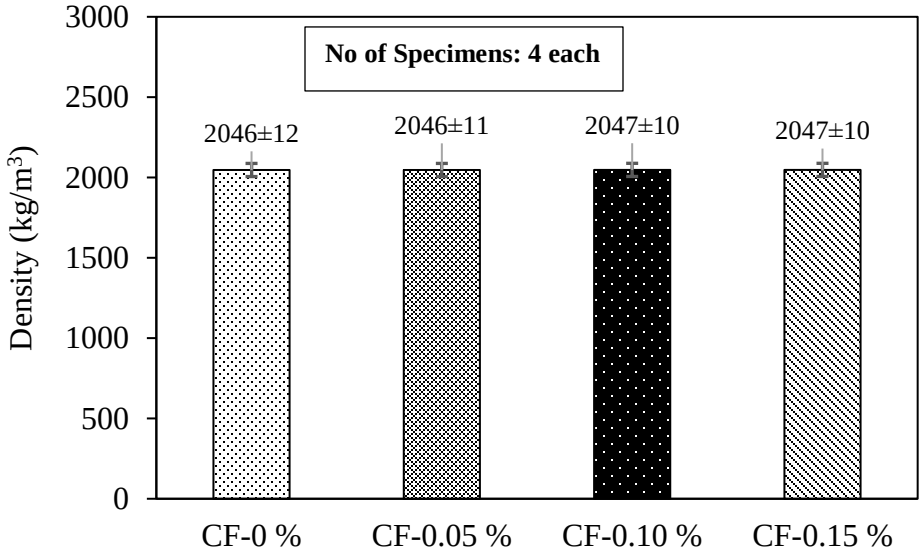

Figure 5-2 Density of smart cement with varying conductive filler contents

As shown in Figure 5-2, the density of smart cement slurry changed by 0.05 % for the smart cements with 0.1 % and 0.15 % of conductive filler contents.

5.3 Density of smart cement with varying salt contents

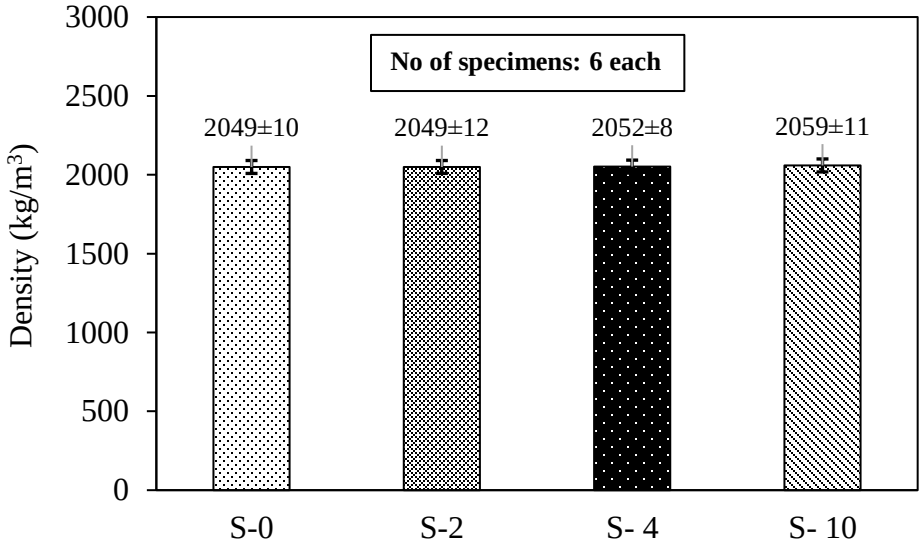

Figure 5-3 Density of smart cement with varying salt contamination

As shown in Figure 5-3, the density of salt-contaminated smart cement slurry changed by 0.2 % and 0.5 % for the smart cements with 4 % and 10 % of salt contents.

5.4 Curing resistivity

5.4.1 Conductive filler

The electrical resistivity of smart cement for varying conductive filler content were measured for one day of curing. Conductive filler content varied from 0-0.15 % of total weight of the composite. The electrical resistivity variation for about 300 mins and 1 day of curing are shown in Figure 5-4 and Figure 5-5 respectively. Control specimen with 0 % of conductive filler showed the highest initial electrical resistivity of 1.06 Ωm and the specimen with 0.15 % of conductive filler showed the lowest initial resistivity of 0.63 Ωm. The electrical resistivity decreased with the increment of conductive fillers. Curing pattern is same for all the specimens. The change in electrical resistivity had occurred due to the conductive behavior of the fillers and cement hydration as well.

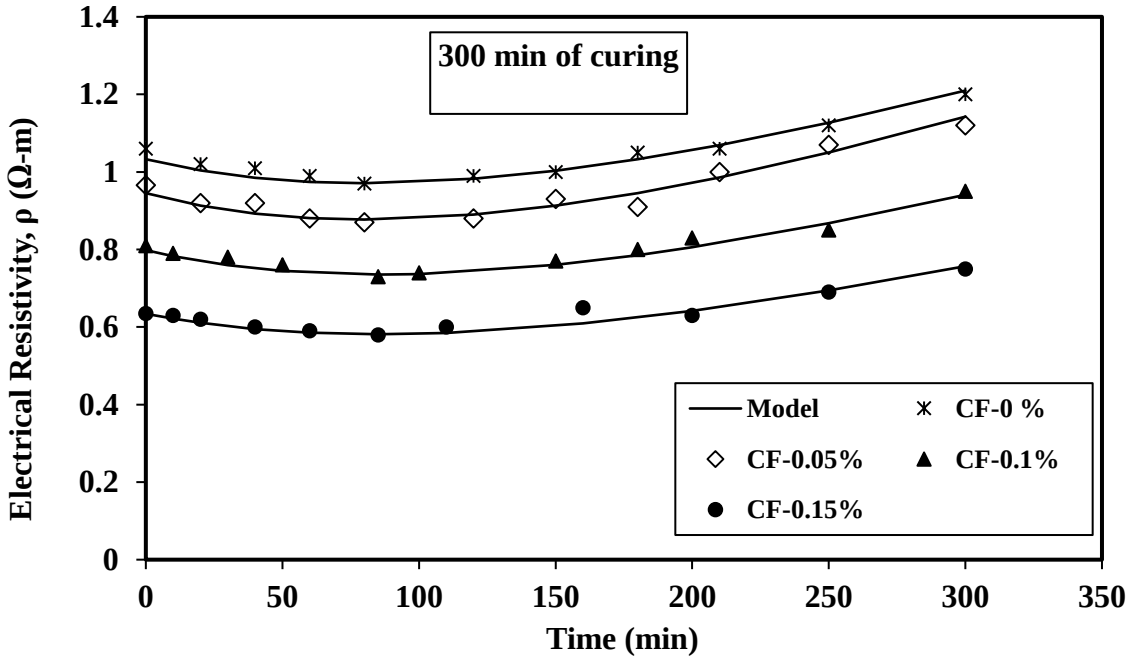

Figure 5-4 Resistivity with conductive filler contents for up to 300 mins of curing

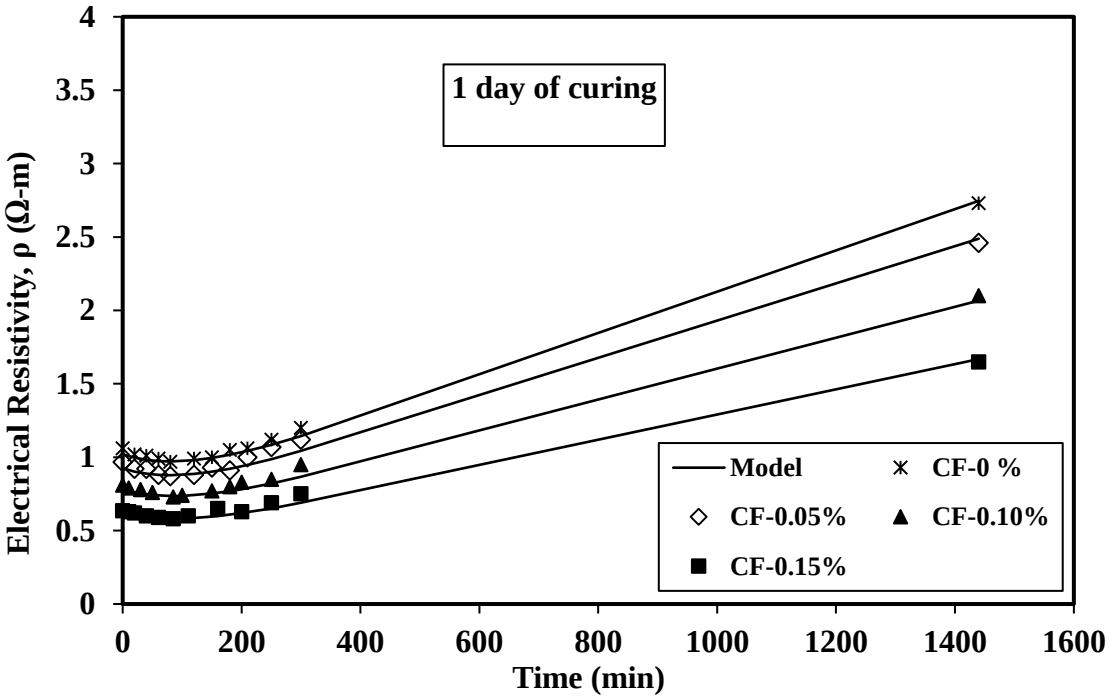

Figure 5-5 Resistivity with conductive filler contents for up to 1 day of curing

Table 5-2 Model parameters of smart cement with conductive filler contents

Conductive filler content (%)	300 min				1 day			
	p_1	q_1	R^2	RMSE	p_1	q_1	R^2	RMSE
CF-0.00	2.3	1.7	0.93	0.02	5.0	1.7	0.98	0.03
CF-0.05	2.5	2.0	0.93	0.02	9.0	2.0	0.96	0.04
CF-0.10	2.6	2.0	0.93	0.01	9.0	2.0	0.96	0.04
CF-0.15	2.6	2.1	0.88	0.01	10.0	2.1	0.95	0.03

The p-q modeling parameters such as p, q, R^2 and RMSE for 300 mins and 1 day of curing are summarized in Table 5-2. The values of p and q increased with the increment of conductive filler contents and the parameter p increased with curing duration as well.

Table 5-3 Resistivity parameters of smart cement with conductive filler contents

Conductive filler content (%)	Resistivity parameters			
	t_{min}	ρ_{min}	ρ_{24}	RI_{24} (%)
CF-0.00	80	0.97	2.73	181
CF-0.05	80	0.87	2.46	183
CF-0.10	85	0.73	2.10	188
CF-0.15	85	0.58	1.65	184

The resistivity parameters are summarized in Table 5-3 and the correlation of t_{min} and ρ_{min} are shown in Figure 5-6 and Figure 5-7. t_{min} is the time duration to reach the minimum resistivity. Parameter ρ_{24} indicates the resistivity after 24 hours of curing. Resistivity index (RI_{24}) is an indicator of cement hydration and curing. Parameters ρ_{min} and ρ_{24} decreased with conductive filler content increase. The t_{min} reduced by 5 mins for the smart cement with conductive filler contents 0.10 % and 0.15 %. The maximum increase in resistivity index (RI_{24}) was 1.6 % for the smart cement with 0.1 % of conductive filler contents. Since RI_{24} did not change significantly, conductive filler did not affect the hydration of smart cement.

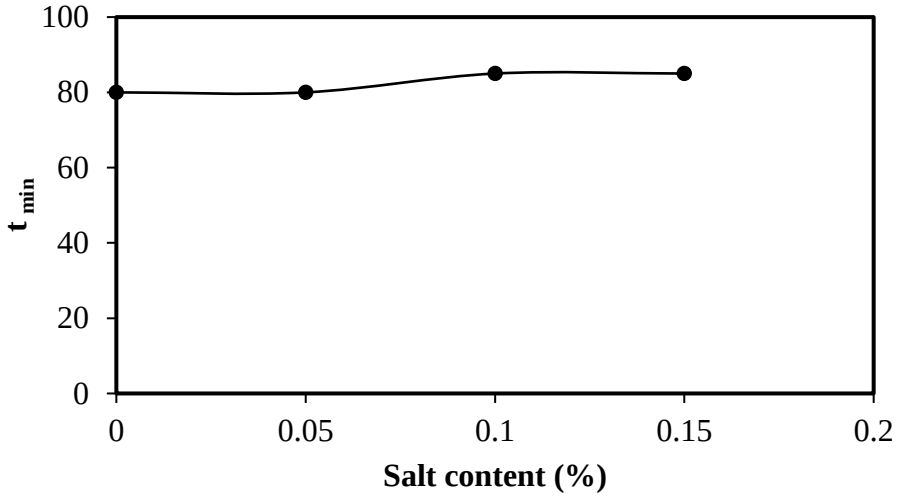

Figure 5-6 Correlation of t_{min} and salt content

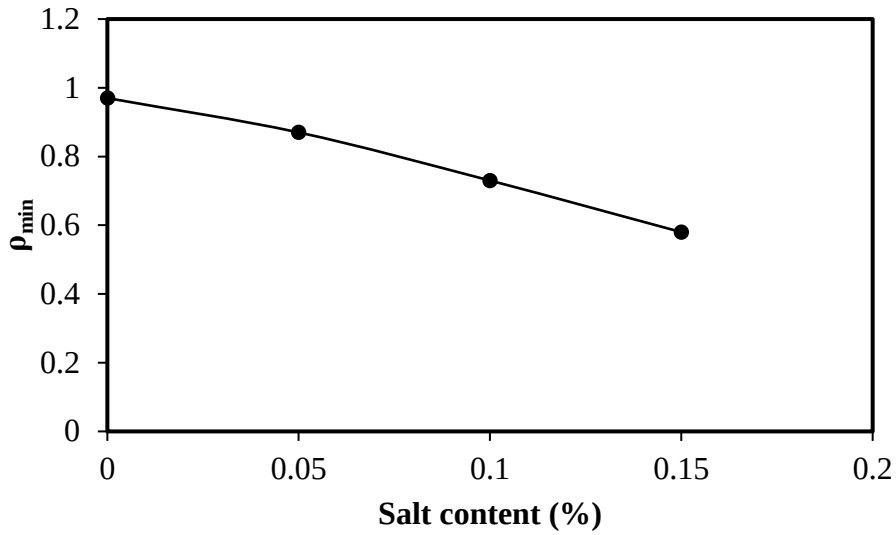

Figure 5-7 Correlation of ρ_{min} and salt content

5.4.2 Salt contamination

The electrical resistivity measurements were taken for a day to characterize the curing and hydration of smart cement with varying salt contents from 0-4 % by weight of water. The electrical resistivity variation for about 300 mins and 1 day of curing are shown in Figure 5-8 and Figure 5-9 respectively. The control specimen without additives had the highest initial resistivity of 1.06 Ωm and the specimen with 4 % of salt content had the lowest initial resistivity of 0.25 Ωm. Due to salt contamination, the initial resistivity of smart cement has been reduced by more than 60 %.

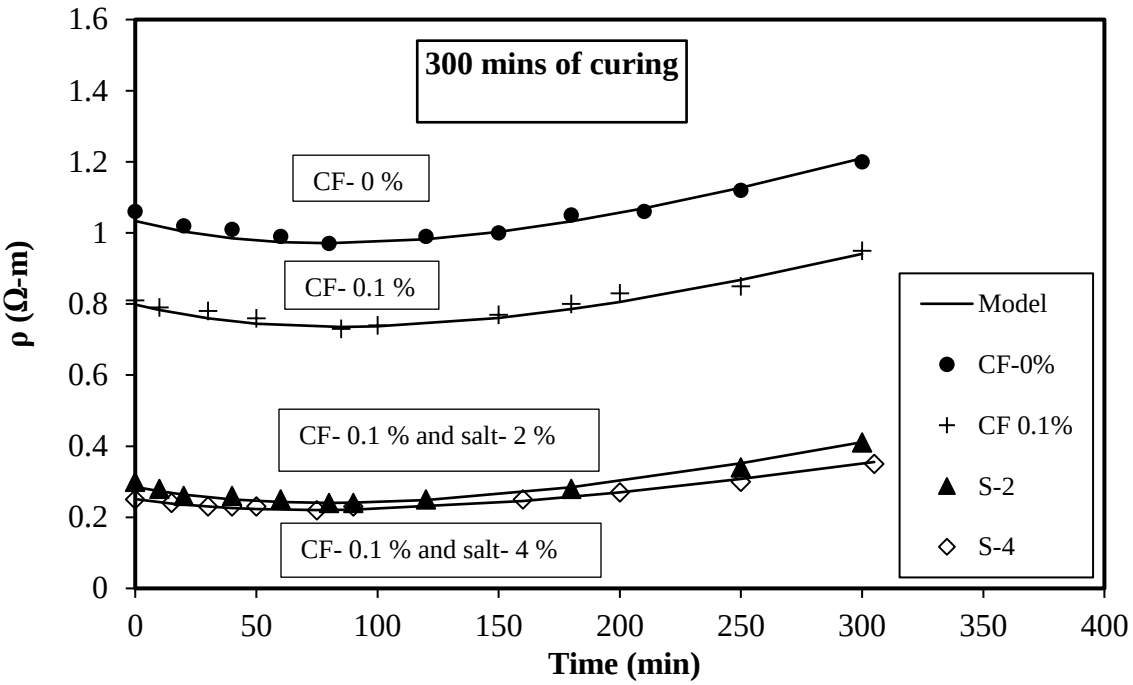

Figure 5-8 Resistivity for varying salt contents for 300 mins of curing

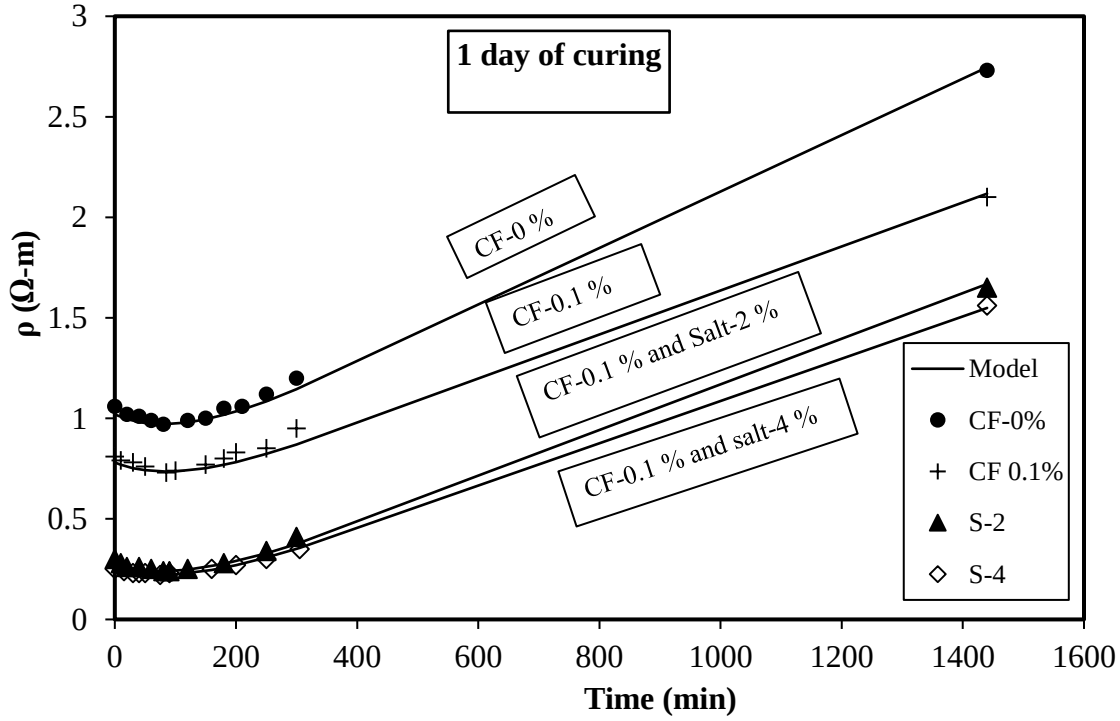

Figure 5-9 Resistivity for varying salt contents for 1 day of curing

The p-q modeling parameters such as p, q, R^2 and RMSE for 300 mins and 1 day of curing are summarized in Table 5-4. The values of p and q increased with the increment of salt contents and the parameter p increased with curing duration as well.

Table 5-4 Model parameters of salt-contaminated smart cement

Conductive filler contents and salt contents (%)	300 min				1 day			
	p_1	q_1	R^2	RMSE	p_1	q_1	R^2	RMSE
CF- 0.00	2.3	1.7	0.93	0.02	5.0	2.0	0.98	0.03
CF- 0.10	2.6	2.0	0.93	0.01	8.0	2.0	0.96	0.03
CF- 0.10, S-2	7.0	5.0	0.97	0.01	12.0	5.0	0.98	0.01
CF- 0.10, S-4	12	5.0	0.97	0.00	12.0	5.0	0.99	0.01

Table 5-5 Resistivity parameters of salt-contaminated smart cement

Conductive filler contents and salt contents (%)	Resistivity Parameters			
	t_{min}	ρ_{min}	ρ_{24}	RI_{24} (%)
CF- 0.00	80	0.97	2.73	181
CF- 0.10	85	0.73	2.10	188
CF- 0.10, S-2	80	0.24	1.65	588
CF- 0.10, S-4	75	0.22	1.56	609

The resistivity parameters are summarized in Table 5-5 and the correlation of t_{min} and ρ_{min} are shown in Figure 5-10 and Figure 5-11. The t_{min} is the time duration to reach the minimum resistivity. The ρ_{24} indicates the resistivity after 24 hours of curing. Resistivity index (RI_{24}) is an indicator of cement hydration and curing. The reduction in t_{min} of salt-contaminated smart cement from 85-80 mins and from 80-75 mins indicates that the hydration was accelerated. Also, the increase in RI_{24} from 188- 588 % and from

588-609 % indicates that the hydration was increased. So it can be concluded that due to the salt contamination, hydration of smart cement was accelerated.

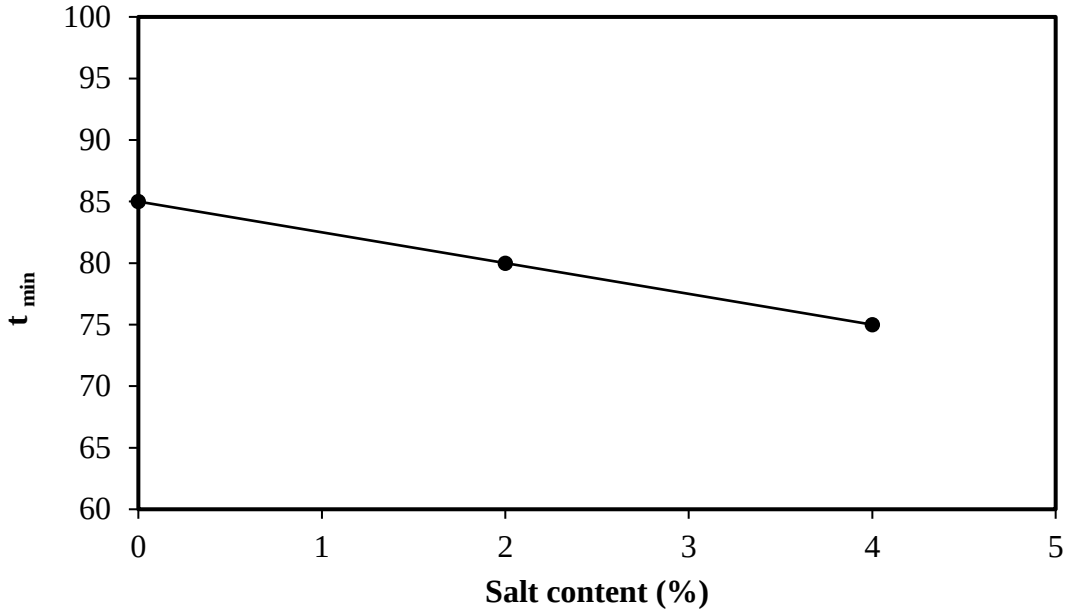

Figure 5-10 Correlation of t_{min} and salt content

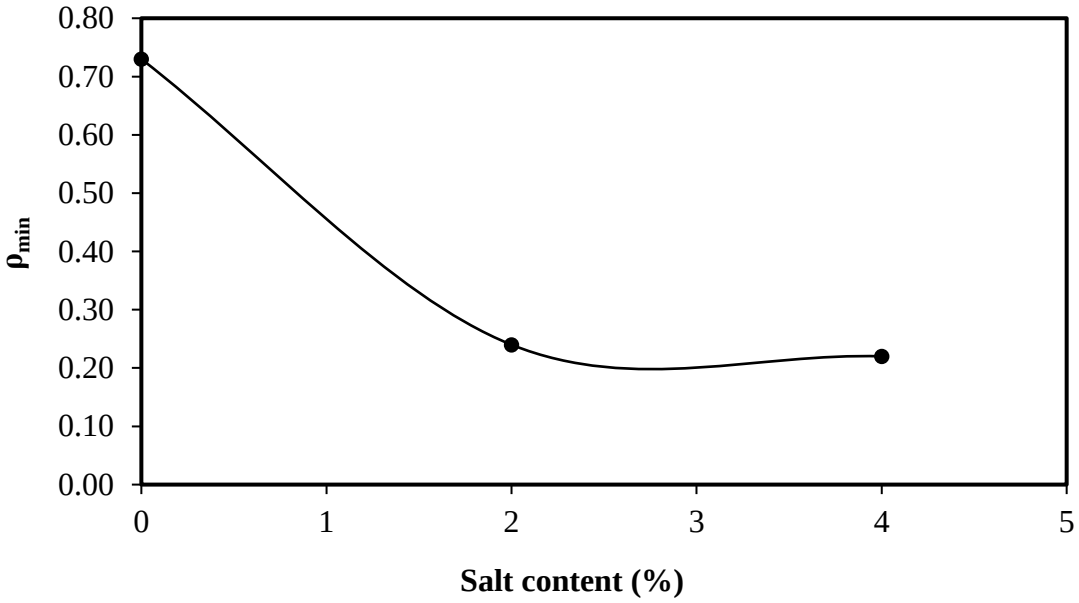

Figure 5-11 Correlation of ρ_{min} and salt content

5.5 Tensile piezo-resistivity of smart cement with conductive filler contents

Smart cement with varying conductive filler contents from 0-0.15 % of total weight was considered for this study. The split tensile test was done after 28 days of curing to avoid resistance change during hydration of cement. The p-q model was used to model and interpret the results. The results obtained for 1-4 and 2-4 probe configurations for loading and unloading were shown in Figure 5-12 and Figure 5-13 respectively.

While piezo-resistivity and tensile stress at failure increased with addition of conductive fillers, the change in resistivity for a particular loading is higher for smart cement with 0.1 % of conductive filler content than that of other specimens. Therefore, the smart cement with 0.1 % of conductive filler content was chosen for further studies.

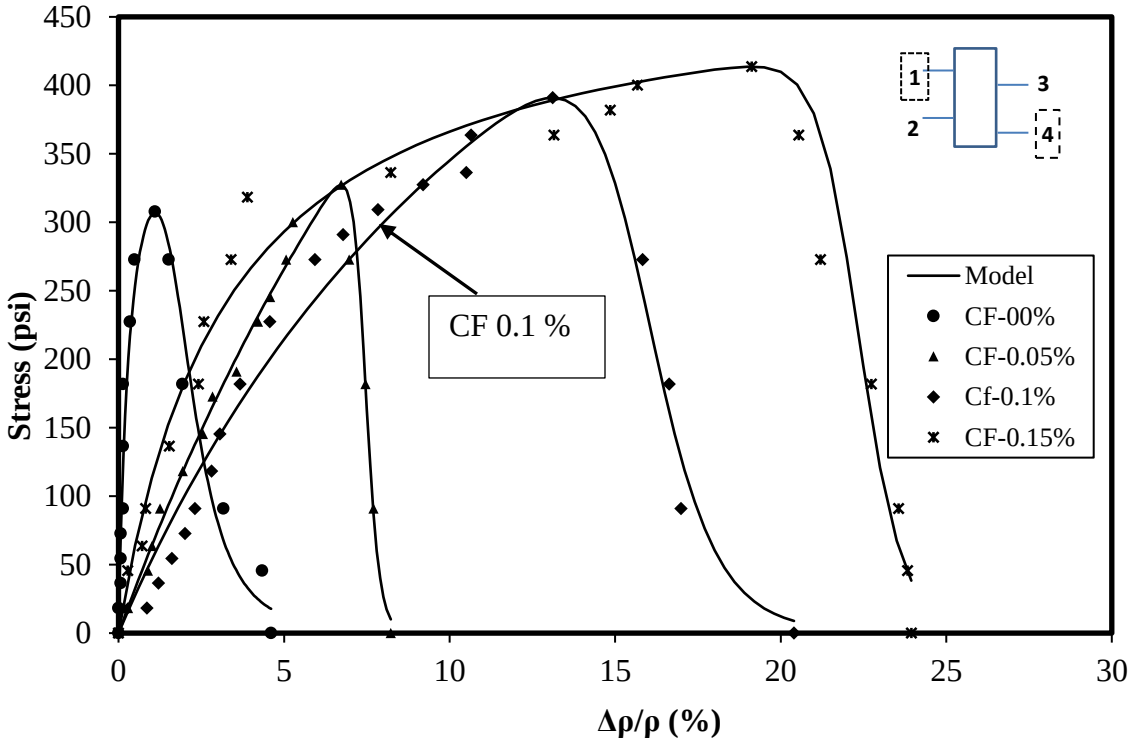

Figure 5-12 Tensile piezo-resistive behavior with CF contents (probe 1-4)

The model parameters, split tensile strength and piezo-resistivity at failure are summarized for probe configurations 1-4 and 2-4 in Table 5-6 and Table 5-7.

Table 5-6 Model parameters of smart cement with CF contents (probe 1-4)

Smart cement	Probe configuration 1-4				Split Tensile Strength (psi)	Piezo-resistivity at failure (%)
	p_2	q_2	R^2	RMSE (psi)		
CF- 0%	0.05	0.22	0.93	25.77	308±8	1
CF- 0.05%	0.02	0.73	0.98	13.10	327±10	7
CF- 0.1%	0.03	0.53	0.97	20.96	391±8	13
CF- 0.15%	0.004	0.15	0.95	30.27	414±12	19

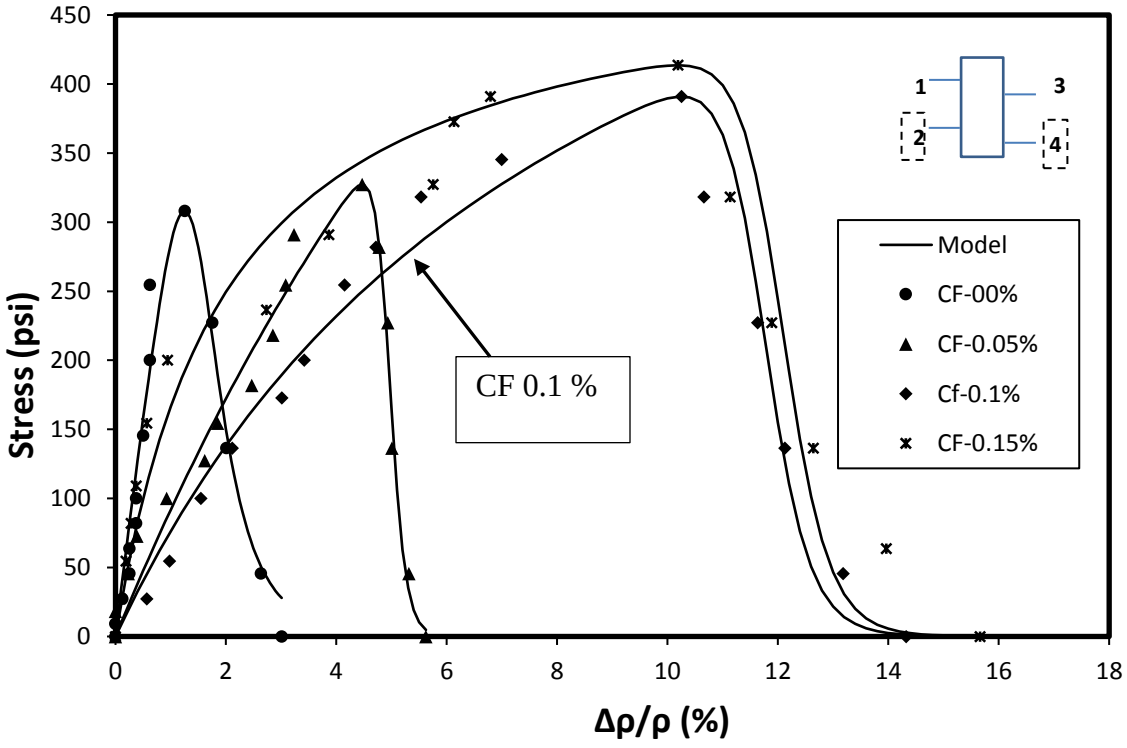

Figure 5-13 Tensile piezo-resistive behavior with CF contents (probe 2-4)

Table 5-7 Model parameters of smart cement with CF contents (probe 2-4)

Smart cement	2-4 Probe configuration				Splitting Tensile Strength (psi)	Piezo-resistivity at failure (%)
	p_2	q_2	R^2	RMSE (psi)		
CF- 0%	0.15	0.74	0.94	24.02	308±8	1
CF- 0.05%	0.02	0.75	0.97	18.26	327±10	4
CF- 0.1%	0.02	0.45	0.96	23.48	391±8	10
CF- 0.15%	0.01	0.16	0.93	36.03	414±12	10

5.6 Direct tensile test for smart oil well cement

5.6.1 Tensile Stress-Strain behavior of smart cement

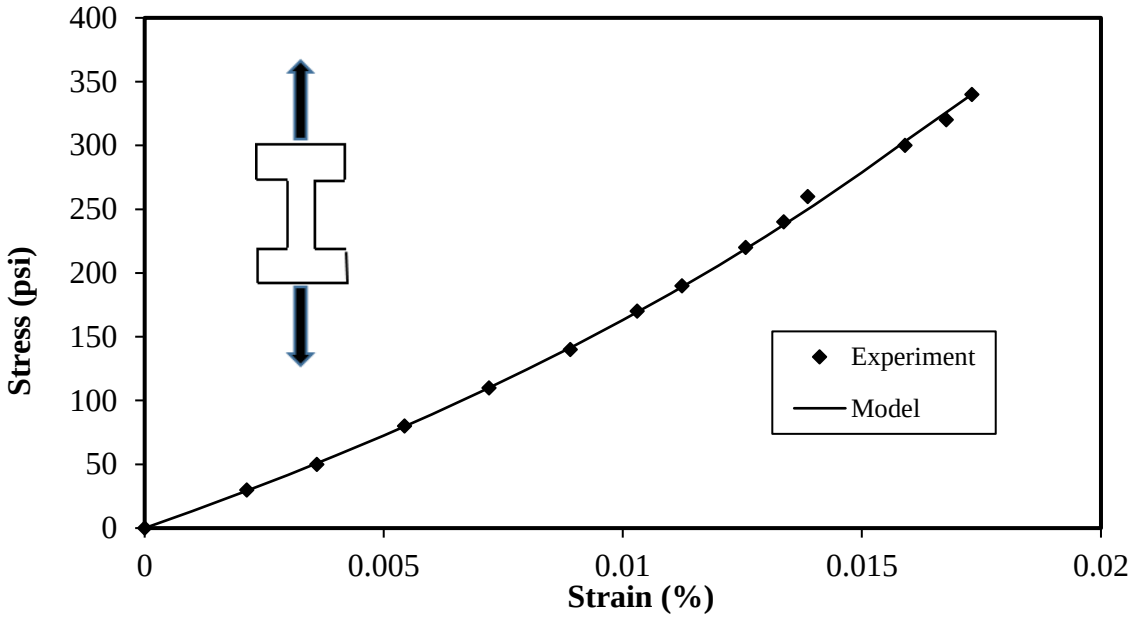

Figure 5-14 Stress vs strain under direct tension of smart cement

Tensile stress of smart cement was 340 psi and the corresponding failure strain was 0.0173 % as shown in the Figure 5-14. Model parameters are summarized in Table 5-8.

Table 5-8 Model parameters of stress-strain behavior

Smart cement	p_0	q_0	R^2	RMSE (psi)	Direct Tension (psi)	Strain at failure (%)
CF 0.1%	0.01	1.50	1.00	3.63	340±10	0.0173

5.6.2 Tensile piezo-resistive behavior of smart cement

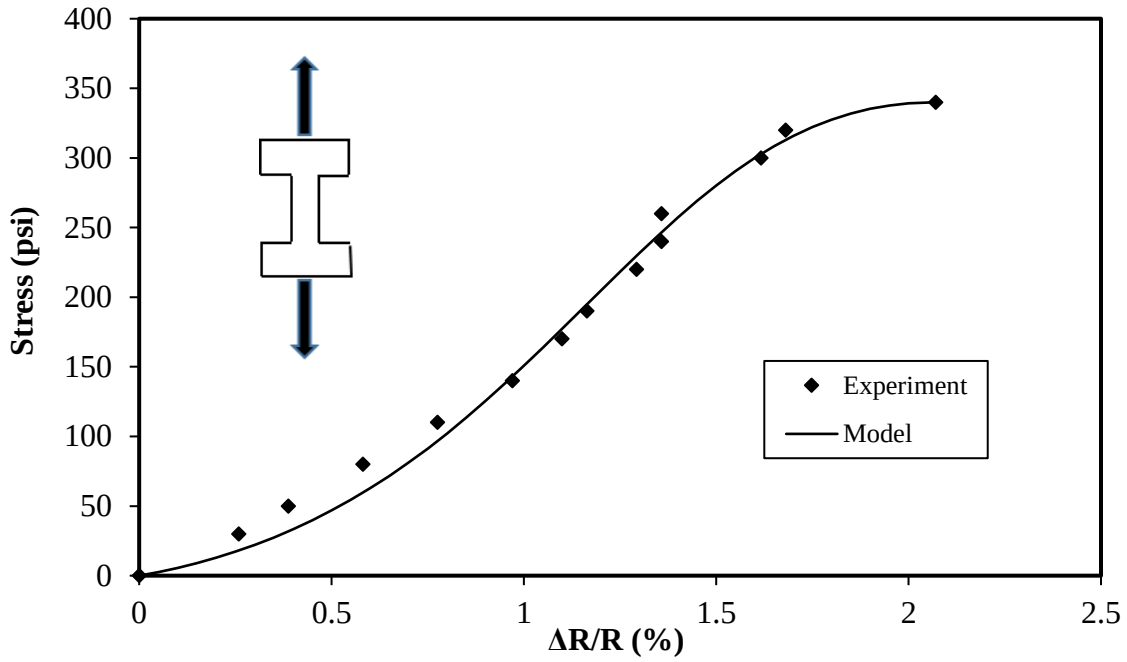

Figure 5-15 Direct tension and piezo-resistivity of smart cement

Since split tensile test is an indirect tensile test, direct tensile test was done to see the accuracy of the split tensile test. Smart cement with 0.1 % of conductive filler was used for the test. After 8 days of curing with 100 % of humidity, direct tensile test was done.

The p-q model was used to model and interpret the results. As shown in the Figure 5-15, the direct tensile stress of the smart cement was 340 psi and corresponding piezo-resistivity was 2.07 % which was 117 times more than the strain.

The model parameters are given in Table 5-9. The root mean square error shows an error of 10 psi in direct tension.

Table 5-9 Model parameters of smart cement under direct tension

Smart cement	**p_2**	**q_2**	**R^2**	**RMSE (psi)**	**Direct Tension (psi)**	**Piezo-resistivity at failure (%)**
CF 0.1%	10.00	3.60	0.99	10.4	340±10	2.07

5.6.3 Comparison of Direct tensile and Split tensile tests

The piezo-resistivity and corresponding split tensile strength of smart cement with 0.1 % conductive filler content were 13 % and 391 psi at failure whereas the piezo-resistivity and corresponding direct tensile strength were 2 % and 340 psi respectively. The tensile strengths were comparable which indicated the reliability of the split tensile test. Due to the variation in the stress distribution and experimental setup, piezo-resistivity was lower for direct tension.

5.7 Tensile piezo-resistivity of smart cement with salt contents

Salt contaminated smart cement was used to study its tensile piezo-resistive behavior, in particular to see the effects of salt contamination in oil well cementing. Since

sea water contains 3.5 % of salts in average, the salt contents used for this study were 2, and 4 % by weight of water. To see the effects of higher amount of salt contamination, 10 % of salt content also was selected for this study. The control smart cement specimen was made without any salt contamination. P-q model was used to predict and interpret the results.

The results obtained for probe configuration 1-4 of salt contaminated smart cement were shown in Figure 5-16.

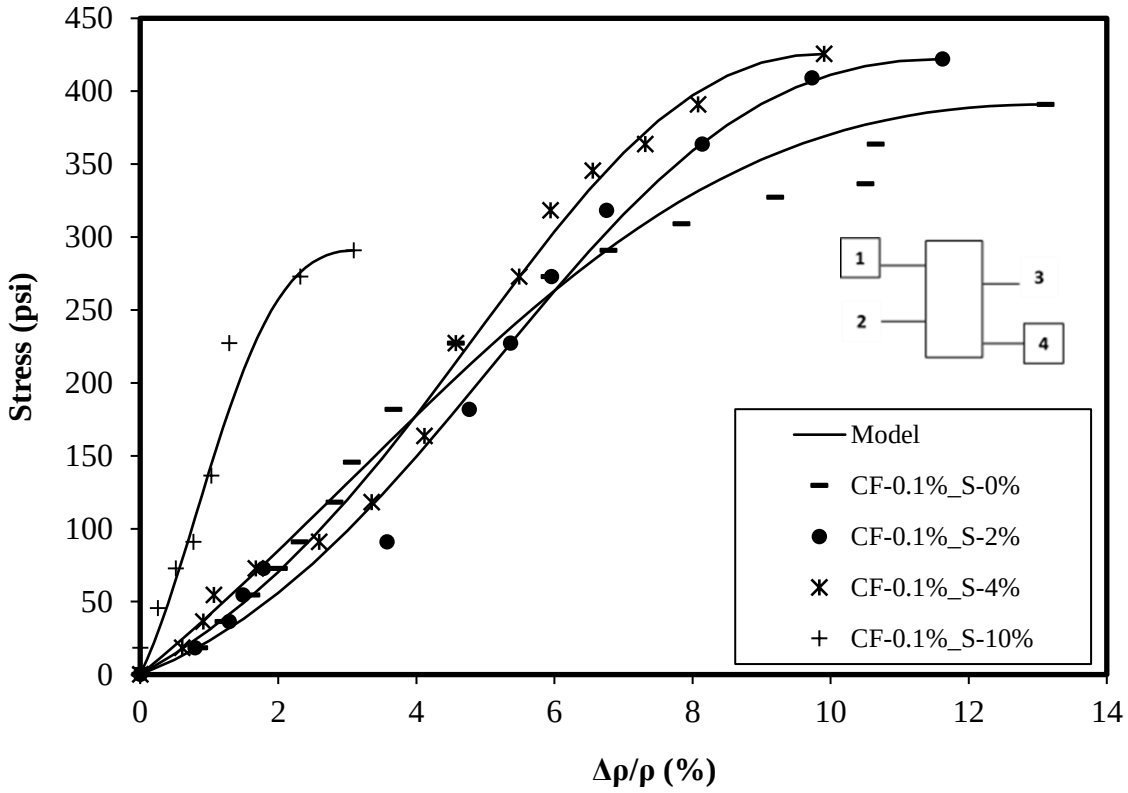

Figure 5-16 Tensile piezo-resistive behavior of salt contaminated smart cement

While the split tensile strength of specimens with 2 and 4 % of salt increased by 31 psi and 4 psi compared to the control specimen, piezo-resistivity decreased by 2 and 3 % respectively as summarized in Table 5-10. In contrast to the results obtained for smart

cement with 2 and 4 % of salt contents, the smart cement with 10 % of salt content decreased the piezo-resistivity and split tensile strength by 10 % and 100 psi respectively compared to the control specimen.

Table 5-10 Model parameters of salt contaminated smart cement (probe 1-4)

Smart cement	Probe configuration 1-4				Splitting Tensile Strength (psi)	Piezo-resistivity at failure (%)
	p_2	q_2	R^2	RMSE (psi)		
S-0	0.84	0.77	0.98	17	391±10	13.12
S-2	25.30	2.06	0.99	14	422±6	11.62
S- 4	1.85	1.63	0.99	12	426±8	9.91
S- 10	4	0.80	0.97	16	291±10	3.09

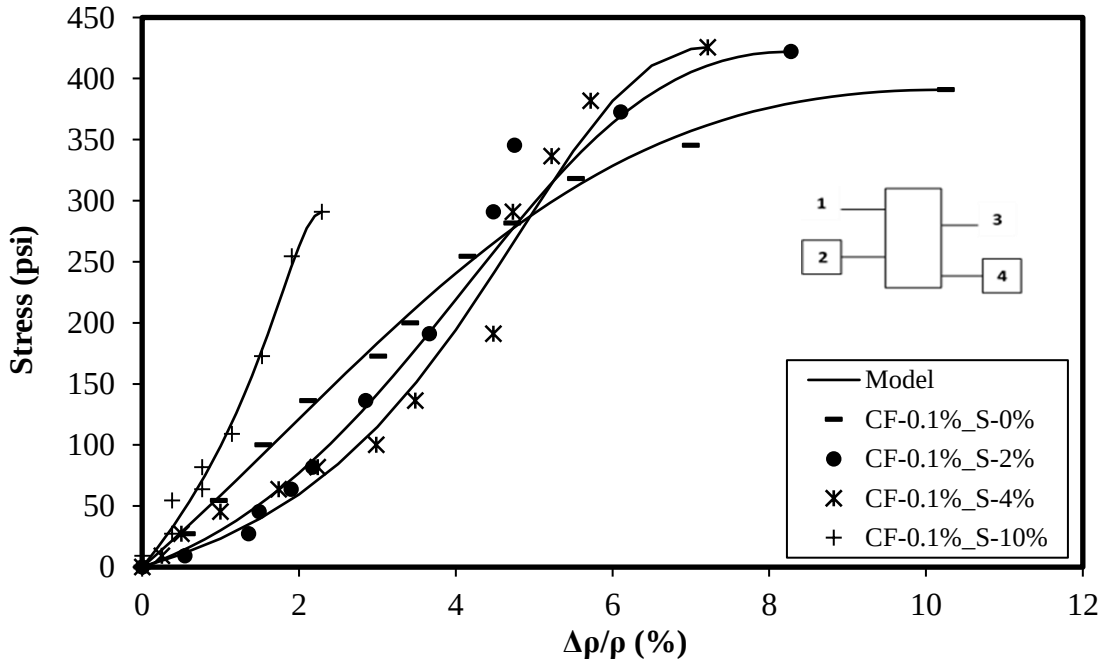

Figure 5-17 Tensile piezo-resistive behavior of salt contaminated smart cement

The results obtained for probe configuration 2-4 of salt contaminated smart cement are shown in Figure 5-17.

As summarized in Table 5-11, from the results obtained for probe configuration 2-4, piezo-resistivity decreased by 2, 3 and 8 % for the smart cements with 2, 4 and 10 % of salt contamination respectively.

Table 5-11 Model parameters of salt contaminated smart cement (probe 2-4)

Smart cement	**Probe configuration 2-4**				**Splitting Tensile Strength (psi)**	**Piezo-resistivity at failure (%)**
	p_2	**q_2**	**R^2**	**RMSE (psi)**		
S-0	0.83	0.69	0.99	6.97	391±10	10.25
S-2	10.00	2.32	0.98	22.40	422±6	8.27
S- 4	2.72	3.17	0.98	20.67	426±8	7.21
S- 10	0.18	1.65	0.99	9.73	291±10	2.29

According to the results obtained in this study, even though lower concentrations of salt contents improve the tensile strength of smart cement, it affects the piezo-resistivity adversely. Higher concentrations of salt contamination in smart cement affect both the piezo-resistivity and tensile strength adversely.

5.8 Correlation between I_1 and J_2

Using the data obtained from direct tensile test, splitting tensile test and compression test, I_1 and J_2 were calculated and correlated as shown in Figure 5-18. The following equation,

$$J_2 = Y_o + \frac{X}{A+BX} \ , \qquad 5\text{-}2$$

proposed by Vipulanandan, was used to predict the experimental results where A and B are model parameters. The model parameters are summarized in Table 5-12.

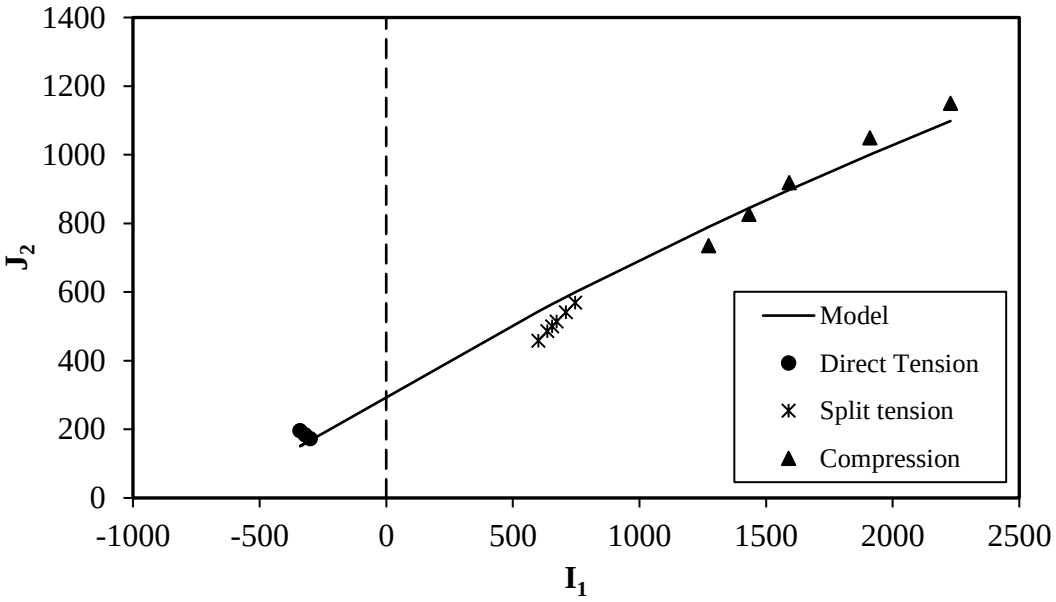

Figure 5-18 Correlation of J_2 and I_1

Table 5-12 Model parameters

Y_0	A	B	R^2	RMSE
300	2.34	0.0002	0.97	49

5.9 Summary

The curing and hydration were characterized with electrical resistivity measurements for a day for smart cement with varying conductive filler contents and salt contents. Direct tension test was done to confirm the reliability of split tension test. Tensile piezo-resistive behavior of smart cement was characterized with both direct tension test data and split tension test data. From the results obtained for this study, the following can be summarized.

1. The density of smart cement slurry changed by 0.05 % for the smart cements with 0.1 % and 0.15 % of conductive filler contents compared to the control cement and the density of salt-contaminated smart cement slurry changed by 0.2 % and 0.5 % for the smart cements with 4 % and 10 % of salt contents.
2. The resistivity index (RI_{24}) of the smart cement with varying conductive filler contents did not change significantly which indicates that conductive filler did not affect the hydration of smart cement.
3. The increase in RI_{24} for the 2 and 4 % of salt contaminated smart cement from 188-588 % and from 588-609 % respectively indicates that the hydration was accelerated compared to control specimen.
4. The smart cement with 0.1 % of conductive filler content is more sensing compared to other smart cements since its resistivity change for a particular load is more than that of other specimens.
5. Lower concentrations of salt contents (2-4 %) improve the tensile strength of smart cement, but it affects the piezo-resistivity adversely. Higher concentrations of salt contamination in smart cement affect both the piezo-resistivity and tensile strength adversely.

CHAPTER 6 POLYMER-ENERGY TREATMENT

In this chapter, polymer-energy treatment of tensile cracks in smart cement was discussed. Since Acrylamide polymer was used as a repair material and energy was supplied by DC supply, this crack repair technique is called the polymer-energy treatment.

The solid cylindrical and hollow cylindrical smart cement specimens, which were deteriorated by split tensile test, were used for the repair to characterize the repair technique. The p-q model was used to predict the tensile piezo-resistive behavior of smart cement after the repair.

6.1 Average total Energy used for the repair of damaged smart cement

Joule's law is

$$Q = I^2 \times R \times t, \qquad 3\text{-}4$$

where Q is total energy, I is electrical current, R is resistance, and t is time. It was used to calculate the average total energy supplied during the crack repair for 7 days. The average total energy used for 7 days was

$$Q = 0.01^2 * (2300+1500+1300+1100+800+700+600) * 24 * 60 * 60$$

$$= 71.7 \text{ kJ}.$$

6.2 Solid cylindrical smart cement

6.2.1 Density of solid smart cement

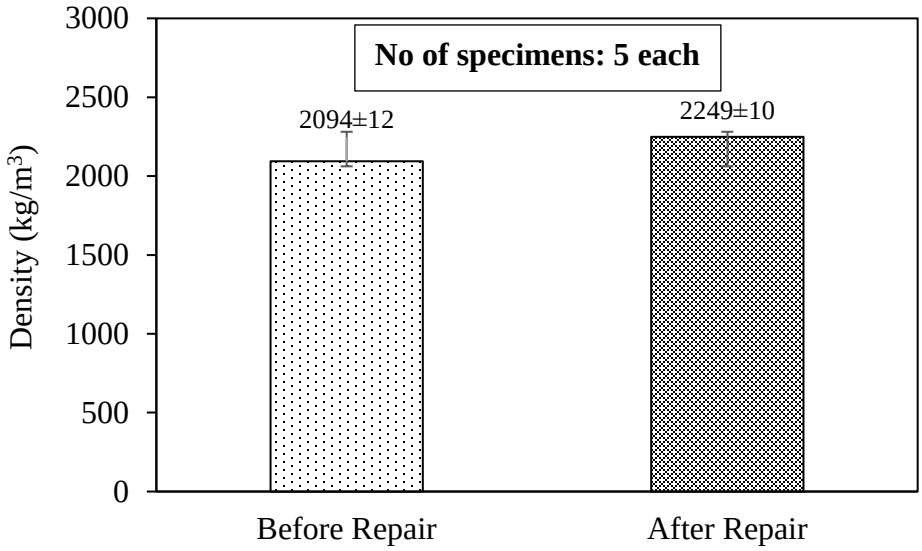

Figure 6-1 Density of solid smart cement before and after repair

The density of damaged specimen before repair was 2094 kg/m^3 and that of repaired specimen was 2249 kg/m^3 as indicated in the Figure 6-1. The 155 kg/m^3 of increment in density occurred due to the polymer-energy treatment.

6.2.2 Electrical Resistivity of solid smart cement

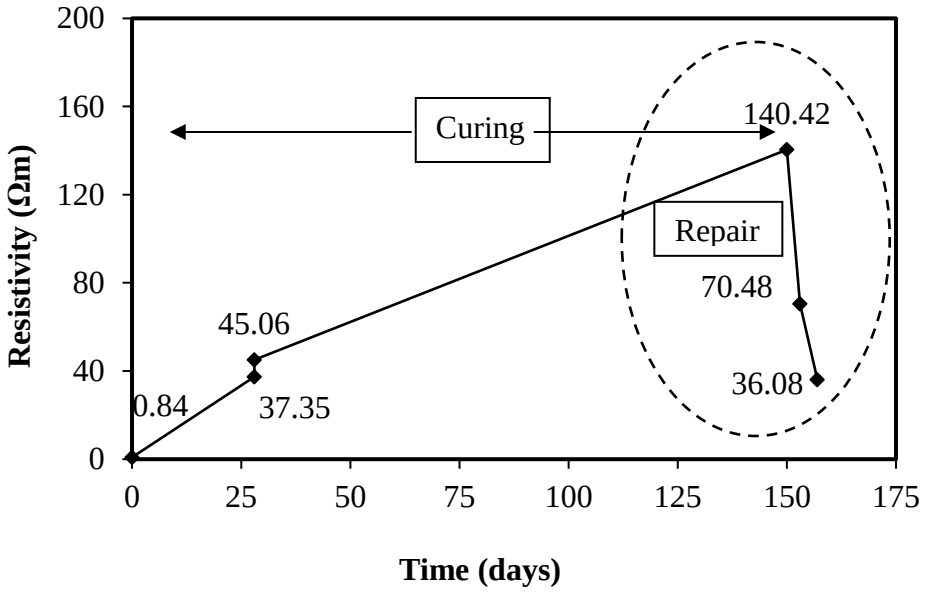

Figure 6-2 Electrical Resistivity of solid smart cement before and after repair

The initial resistivity of fresh smart cement slurry was 0.84 Ωm. After 28 days of curing, split tensile test was done and the resistivity before and after the test was 37.35 Ωm and 45.06 Ωm respectively. The resistivity of damaged specimen at 150 days, before repair, was 140.42 Ωm. After 3 and 7 days of polymer-energy repair, the resistivity went down to 70.48 Ωm and 36.08 Ωm respectively. The sudden drop of resistivity, as indicated in the Figure 6-2, during repair was an indicator of crack healing.

6.2.3 Tensile piezo-resistive behavior of solid smart cement

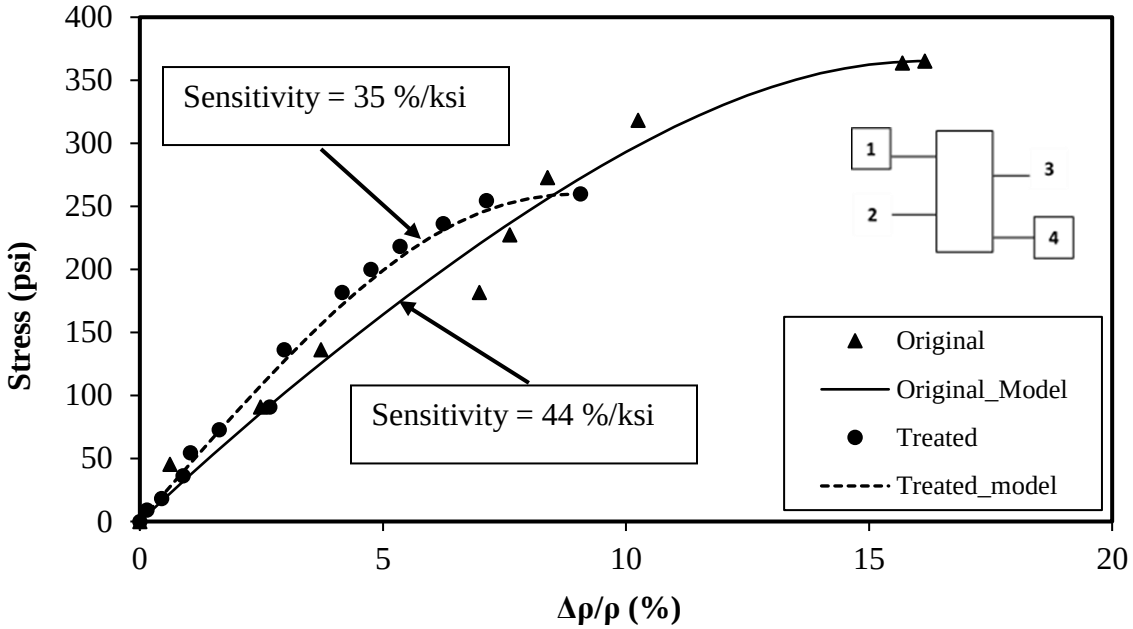

Figure 6-3 Piezo-resistive behavior of solid original and treated specimen

The piezo-resistive behavior of original and polymer-energy treated solid specimens were shown in Figure 6-3. While the split tensile strength obtained for original and treated smart cement were 365 and 260 psi, piezo-resistivity obtained for original and treated smart cement were 16 and 9 % respectively. The repaired specimen has recovered its 56 % of piezo-resistivity and 71 % of split tensile strength.

Model parameters of p-q modeling are summarized in Table 6-1. The material parameters, p and q, increased for repaired smart cement compared to the original specimen.

Table 6-1 Model parameters of solid smart cement before and after repair

Smart cement	Probes 1-4 configuration				Splitting Tensile Strength (psi)	Piezo-resistivity at failure (%)
	p_2	q_2	R^2	RMSE		
Before repair	0.16	0.62	0.98	17	365±8	16
After repair	0.3	0.64	0.99	9	259±10	9

6.3 Hollow cylindrical smart cement

6.3.1 Density of hollow smart cement

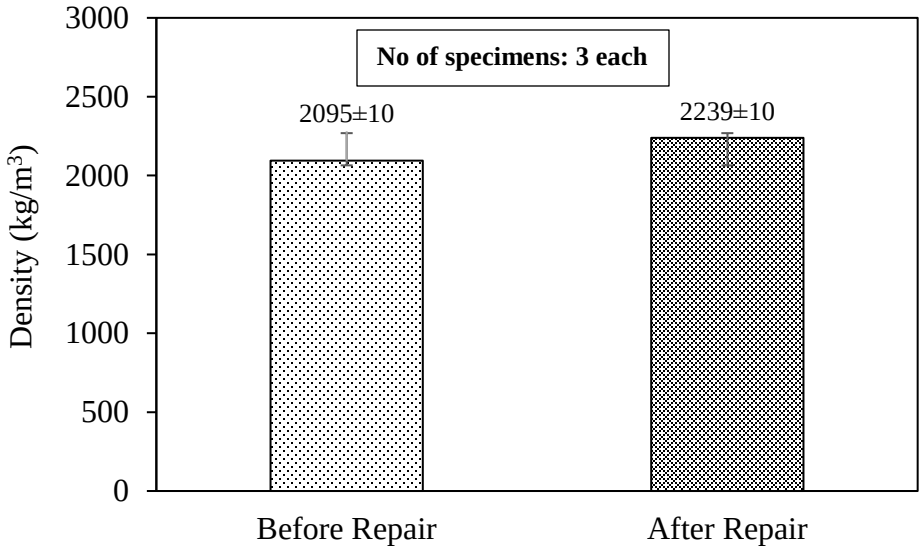

Figure 6-4 Density of hollow smart cement before and after repair

The density of damaged specimen before repair was 2095 kg/m^3 and that of repaired specimen was 2239 kg/m^3 as indicated in the Figure 6-4. The 144 kg/m^3 of increment in density occurred due to the polymer-energy treatment.

6.3.2 Electrical Resistivity of hollow smart cement

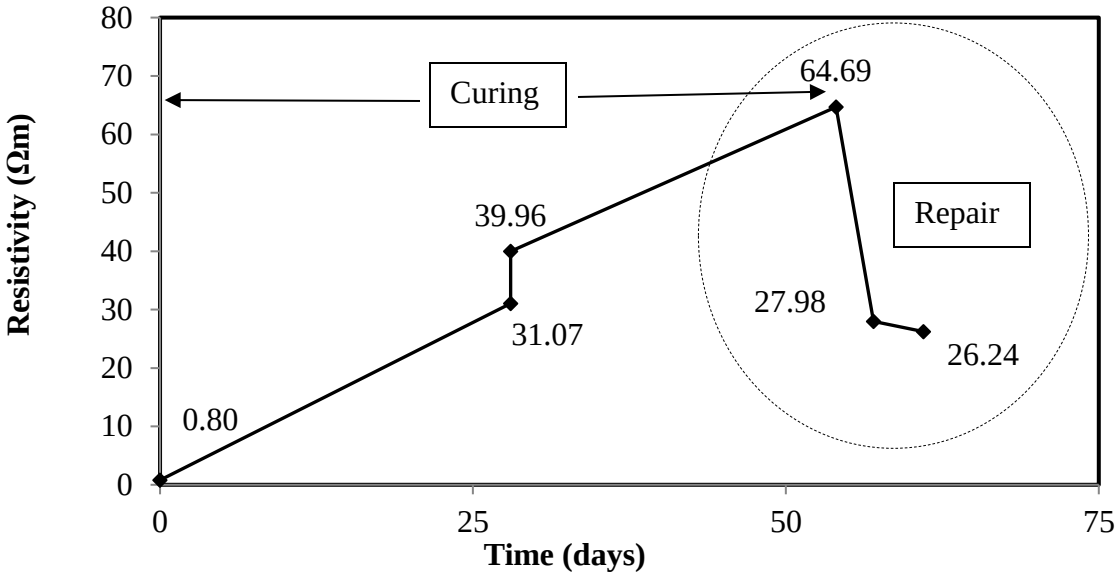

Figure 6-5 Electrical Resistivity of hollow smart cement before and after repair

The initial resistivity of fresh smart cement slurry was 0.80 Ωm. After 28 days of curing, split tensile test was done and the resistivity before and after the test was 31.07 Ωm and 39.96 Ωm respectively. The resistivity of damaged specimen at 54 days, before repair, was 64.69 Ωm. After 3 and 7 days of polymer-energy repair, the resistivity went down to 27.98 Ωm and 26.24 Ωm respectively. The sudden drop of resistivity, as indicated in the Figure 6-5, during repair was an indicator of crack healing.

6.3.3 Tensile piezo-resistive behavior of hollow smart cement

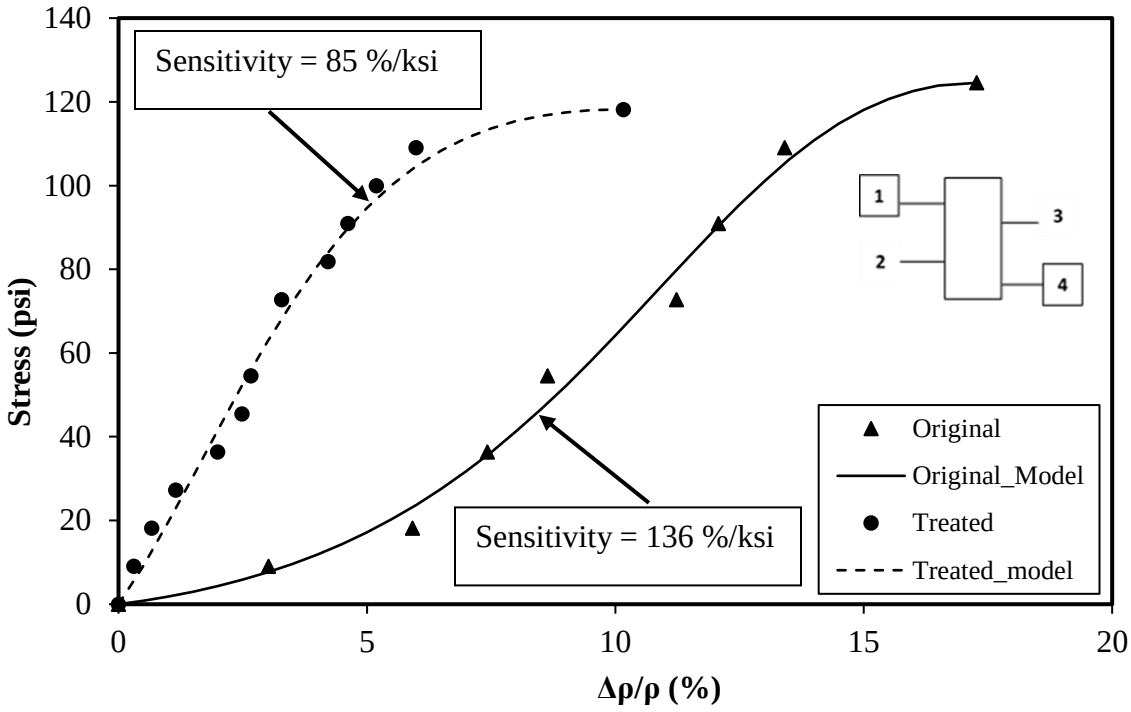

Figure 6-6 Piezo-resistive behavior of hollow original and treated specimen

The piezo-resistive behavior of original and polymer-energy treated hollow specimens were shown in Figure 6-6. While the split tensile strength obtained for original and treated smart cement were 125 and 118 psi, piezo-resistivity obtained for original and treated smart cement were 17 and 10 % respectively. The repaired specimen has recovered its 59 % of piezo-resistivity and 95 % of its split tensile strength.

Model parameters of p-q modeling are summarized in Table 6-2. The material parameters, p and q, increased for repaired smart cement compared to the original specimen.

Table 6-2 Model parameters of hollow smart cement before and after repair

Smart cement	Probes 1-4 configuration				Splitting Tensile Strength (psi)	Piezo-resistivity at failure (%)
	p_2	q_2	R^2	RMSE		
Original	88.35	4.98	0.99	3.88	125±5	17.27
Treated	6.44	0.71	0.99	3.87	118±5	10.16

6.4 Discussion of the results obtained for repaired solid and hollow smart cement

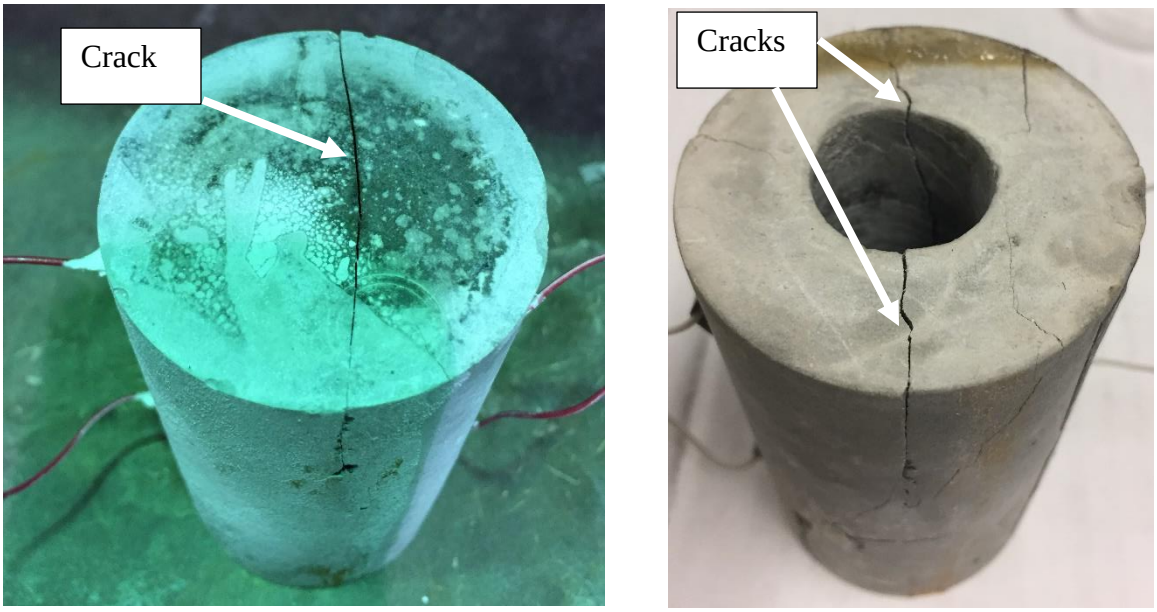

(a) (b)

Figure 6-7 Failed specimens after split tensile test (a) Solid (b) Hollow

The change in density for both the specimens was 7 % increase and occurred due to the polymer absorption. Another indicator of polymer absorption and crack healing was the sudden drop of resistivity during repair of the specimens. The recovery of piezo-resistivity and split tensile strength for solid smart cement due to polymer-energy treatment

were 56 % and 71 % of its original solid smart cement whereas that of hollow specimen were 59 % and 95 % respectively.

As shown in Figure 6-7 (a) and (b), hollow specimen deformed more than solid specimen due to its split and flexure modes of failures and solid specimen failed due to its split mode of failure.

6.5 Summary

From the experimental results obtained from the polymer-energy treatment of solid and hollow smart cement, the following can be summarized.

1. The change in density for both solid and hollow specimens after the repair of the crack resulted in 7 % increase and occurred due to the penetration of the polymer in to the smart cement.
2. Another indicator of polymer penetration and crack healing was the sudden drop of resistivity during repair of the specimens.
3. The recovery of piezo-resistivity and split tensile strength for solid smart cement due to polymer-energy treatment were 56 % and 71 % of its original solid smart cement whereas that of hollow specimen were 59 % and 95 % respectively.

CHAPTER 7 CONCLUSIONS AND RECOMMENDATIONS

This study focused mainly on rapid polymer stabilization of synthetic and natural expansive soils, tensile piezo-resistivity of smart cement and salt contaminated smart cement, and polymer-energy treatment of cracks in damaged smart cement. The major findings and recommendations are summarized in section 7.1 and 7.2.

7.1 Conclusions

1. The rapid stabilization of dry synthetic clay (Kaolinite-95 % and Bentonite 5 %) using acrylamide polymer reduced plasticity index by 49 %, swell potential by 88 %, and swell pressure by 21 %.

2. The natural clay obtained from field also justified the efficiency of the acrylamide polymer on expansive soil treatment with a 35 % of reduction in its plasticity index.

3. Even though split tensile test is an indirect tension test method, the tensile strength values obtained were reliable and comparable with direct tensile strength.

4. Among the sensitivities obtained for smart cements with varying conductive filler contents, for a particular stress, the smart cement with 0.1 % of conductive filler content was more piezo-resistive than other specimens.

5. The sensitivity and split tensile strength of smart cement with 2 and 4 % of salt contents were not affected significantly whereas that of smart cement with 10 % of salt content affected adversely.

6. Polymer-energy treatment of damaged smart cement recovered a range 56-59 % of piezo-resistivity and 71-95 % of splitting tensile strength of its original specimen due to its crack healing effect.

7. The p-q model predicted the curing of smart cement in terms of electrical resistivity and the piezo-resistive behavior of smart cement when loading and unloading precisely.

7.2 Recommendations

1. Rapid polymer treatment of natural expansive soil can be done for various natural expansive soils which have varying initial moisture contents to find out the optimum polymer content to be used in field.
2. The effect of temperature on rapid polymer stabilization of expansive soil can be explored for the field application of this technique.
3. Characterization of polymer treatment on expansive soils can be done with electrical resistivity measurements.
4. Compressive behavior of smart cement can be considered for the characterization of polymer-energy treatment of damaged smart cement.

References

1. Azzam, W (2010), "Reduction of the Shrinkage-Swelling Potential with Polymer Nanocomposite Stabilization," *Journal of Applied Polymer Science*, Vol-123, 299-306.
2. Buhler, R and Cerato, A (2007), "Stabilization of Oklahoma Expansive soils Using Lime and Class F Fly Ash," *Problematic soils and Rocks and In situ Characterization*, GSP 162, 1-10.
3. Chang, I, Im, J and Cho, G (2016), "Introduction of Microbial Biopolymers in Soil Treatment for Future Environmentally-Friendly and Sustainable Geotechnical Engineering," *Sustainability*, Vol-8, 1-23.
4. Choi, Y and Yuan, R (2005), "Experimental Relationship between Splitting Tensile Strength and Compressive Strength of GFRC and PFRC," *Cement and Concrete Research*, Vol-35, 1587-1591.
5. Dias, D, Thaumaturgo, C (2005), "Fracture Toughness of Geopolymeric Concretes Reinforced with Basalt Fibers," *Cement and Concrete Composites*, Vol-27, 49-54.
6. Gromko, G (1974), "Review of Expansive Soils," *Journal of Geotechnical Engineering Division*, Vol-100, 667-687.
7. Inyang, H, Bae, S, Mbamalu, G and Park, S (2007), "Aqueous Polymer Effects on Volumetric Swelling of Na-Montmorillonite," *Journal of Materials in Civil Engineering*, Vol-19(1), 84-90.
8. Jacobsen, S and Sellevold, E (1996), "Self Healing of High Strength Concrete after Deterioration by Freeze/Thaw," *Cement and Concrete Research*, Vol-26, 55-62.

9. Jefferson, A, Joseph, C, Lark, R, Isaacs, B, Dunn, S and Weager, B (2010), "A New System for Crack Closure of Cementitious Materials Using Shrinkable Polymers," *Cement and Concrete Research*, Vol-40, 795-801.
10. Kan, Y, Yen, T and Lee, M (2008), "Restored Strength of Cracked Concrete Beam Repaired by Epoxy and Polymethyl Methacrylate," *ACI Materials Journal*, Vol-105, 451-458.
11. Li, V, Lim, Y and Chan, Y (1998), "Feasibility Study of a Passive Smart Self-healing Cementitious Composite," *Composites Part B*, Vol-29, 819-827.
12. Liu, J, Shi, B, Jiang, H, Huang, H, Wang, G and Kamai, T (2011), "Research on the Stabilization Treatment of Clay Slope Topsoil by Organic Polymer Soil Stabilizer," *Engineering Geology*, Vol-117, 114-120.
13. Maslehuddin, M, Page, C.L and Rasheeduzzafar (1996), "Effect of Temperature and Salt Contamination on Carbonation of Cements," *Journal of Materials in Civil Engineering*, Vol-8(2), 63-69.
14. Ming, L, Meng, L, Yuanyi, Y, Zaoyuan, L and Xiaoyang, G (2015), "Mechanical Properties of Oil Well Cement Stone Reinforced with Hybrid Fiber of Calcium Carbonate Whisker and Carbon Fiber," *Petroleum Exploration and Development*, Vol-42, 104-111.
15. Mirzababaei, M, Yasrobi, S and Al-Rawas, A (2008), "Effect of Polymers on Swelling Potential of Expansive Soils," *Proceedings of the Institution of Cicil Engineers*, Vol-162, 111-119.
16. Mohammed, A and Vipulanandan, C (2013), "Compressive and Tensile Behavior of Polymer Treated Sulfate Contaminated CL Soil," *Geotech Geol Eng*, Vol-32, 71-83.

17. Mousavi, F, Abdi, E and Rahimi, H (2013), "Effect of Polymer Stabilizer on Swelling Potential and CBR of Forest Road Material," *KSCE Journal of Civil Engineering*, Vol-18, 2064-2071.
18. Naeini, S, Naderinia, B and Izadi, E (2011), "Unconfined Compressive Strength of Clayey Soils Stabilized with Waterborne Polymer," *KSCE Journal of Civil Engineering*, Vol-16(6), 943-949.
19. Oluokun, F, Burdette, E, and Deatherage, J (1991), "Splitting Tensile Strength and Compressive Strength Relationship at Early Ages," *ACI materials journal*, Vol-88, 115-123.
20. Qian, S, Zhou, J, Rooij, M, Schlangen, E, Ye, G and Breugel, K (2009), "Self-Healing Behavior of Strain Hardening Cementitious Composites Incorporating Local Waste Materials," *Cement and Concrete composites*, Vol-31, 613-621.
21. Ryu, J and Otsuki, N (2002), "Crack Closure of Reinforced Concrete by Electrodeposition Technique," *Cement and Concrete Research*, Vol-32, 159-164.
22. Siddique, R (2003), "Effect of Fine Aggregate Replacement with Class F Fly Ash on the Mechanical Properties of Concrete," *Cement and Concrete Research*, Vol-33, 539-547.
23. Sim.J, Park, C and Moon, D.Y, (2005), "Characteristic of Basalt Fiber as a Strengthening Material for Concrete Structures," *Composites: Part B: Engineering*, Vol-36, 504-512.
24. Simao, C, Miranda, C, Vargas, A.A, Pereira, R, Santos, R, Soares, M and Conceicao, A (2012), "Cementing in front of Soluble Salt Zones," *SPE International*, 1-21.

25. Teodoriu, C and Asamba, P (2015), "Experimental Study of Salt Content Effect on Class G Cement Properties with Application to Well Integrity," *Journal of Natural Gas Science and Engineering*, Vol- 24, 324-329.
26. Vipulanandan, C (2014), "Development of Smart Cement for Real Time Monitoring of Ultra-Deep-Water Oil Well Cementing Applications," *CIGMAT-2014 Conference & Exhibition*, 1-16.
27. Vipulanandan, C and Garas, V (2008), "Electrical Resistivity, Pulse Velocity and Compressive Properties of Carbon Fiber Reinforced Cement Mortar," *Journal of Materials in Civil Engineering*, Vol-20:2, 93-101.
28. Vipulanandan, C and Paul, E (1993), "Characterization of Polyester Polymer and Polymer Concrete", *Journal of Materials in Civil Engineering*, Vol-5(1), 62-82.
29. Vipulanandan, C and Prashanth, P (2013), "Impedance Spectroscopy Characterization of a Piezoresistive Structural Polymer Composite Bulk Sensor," *Journal of Testing and Evaluation*, Vol- 41, 898–904.
30. Wafa, F and Ashour, S (1992), "Mechanical Properties of High Strength Fiber Reinforced Concrete," *ACI Materials Journal*, Vol- 89, 449-454.
31. Wang, X, Fu, X and Chung, D (1998), "Strain Sensing Using Carbon Fiber," *Journal of Materials Research*, Vol-14, 790-802.
32. Xie, P, Gu, P (1996), "Electrical Percolation Phenomena in Cement Composites Containing Conductive Fibers," *Journal of Materials Science*, Vol-31, 4093-4097.
33. Yazdandoust, F and Yasrobi, S.S (2010), "Effect of Cyclic Wetting and Drying on Swelling Behavior of Expansive Clays," *Applied Clay Science*, Vol-50, 461-468.

34. Zain, M, Mahmud, H, Ilham, A and Faizal, M (2002), "Prediction of Splitting Tensile Strength of High-Performance Concrete," *Cement and Concrete Research*, Vol-32, 1251-1258.

35. Zanotti, C, Borges, P, Bhutta, A and Banthia, N (2017), "Bond Strength Between Concrete Substrate and Metakaolin Geopolymer Repair Mortar: Effect of Curing Regime and PVA Fiber Reinforcement," *Cement and Concrete Composites*, Vol-80, 307-316.

36. Zhou, X, Lin, X, Huo, M and Zhang, Y (1996), "The Hydration of Saline Oil-Well Cement," *Cement and Concrete Research*, Vol-26, 1753-1759.